Modulating System xc- Activity As A Treatment For Epilepsy

Oscar Alcoreza Jr.

Dissertation submitted to the faculty of the Virginia Polytechnic Institute and State University in partial fulfillment of the requirements for the degree of

Doctor of Philosophy
In
Translational Biology, Medicine, and Health

Harald Sontheimer, Chair
Susan Campbell
Aashit Shah
Michelle Olsen

May 3rd, 2021
Roanoke, VA

Keywords: System xc, epilepsy, astrogliosis, astrocyte, sulfasalazine

Modulating System xc- Activity As A Treatment For Epilepsy

Oscar Alcoreza Jr.

Academic Abstract

Epilepsy is a neurological disorder that presents a significant public health burden, with an estimated five million people being newly diagnosed each year [1]. However, current therapeutics designed to modify neuronal processes, provide no relief to 1-in-3 epileptic patients [2]. Additionally, no disease modifying therapies currently exist to treat the underlying pathological processes involved in epileptogenesis. The overarching goal of this project is to further characterize the role astrocytes play in epileptogenesis, in hopes of revealing novel therapeutic targets to benefit patients who otherwise have no effective treatment options. System xc- (SXC), a cystine/glutamate antiporter expressed in astrocytes, is one such target that has been shown to play a critical role in establishing ambient extracellular glutamate levels in both health and disease. SXC has been shown to play a major role in setting ambient glutamatergic tone in the central nervous system (CNS) as pharmacological inhibition of SXC, using (S)-4-carboxyphenylglycine (S-4-CPG) or antisense xCT, resulted in a 60% reduction in extrasynaptic glutamate in the nucleus accumbens[3,4]. Additionally, investigations in tumor-associated epilepsy revealed that overexpression of SXC seen in glioblastomas lead to higher levels of peritumoral glutamate, neuronal excitotoxicity, and ultimately seizures [5-7]. These studies also found that SXC inhibition with sulfasalazine (SAS), an FDA approved drug and potent inhibitor of SXC, can ameliorate seizure burden in a glioblastoma mouse model. Therefore, the principal objective of this study is to further investigate the role of astrocytic SXC activity in epileptogenesis and seizure generation. In doing so, we also evaluated the efficacy of SAS in reducing seizure burden *in vivo* using an astrogliosis-mediated epilepsy mouse model. In this dissertation we show

that (1) SXC inhibition, using SAS, is able to decrease induced epileptiform activity in multiple models of chemically induced hyperexcitability (2) this is due to a preferential decrease of NMDAR-mediated currents and (3) SXC inhibition, via SAS, decreases seizure burden *in vivo* in an astrogliosis-mediated epilepsy model.

General Audience Abstract

Epilepsy, characterized by unpredictable seizures, affects approximately 2.2 million Americans, with 150,000 new cases being diagnosed each year. Seizures typically occur when there is an imbalance between the excitatory and inhibitory processes in the brain. Because neurons are the primary cell in the brain that carry out these processes, clinically used anti-epileptic drugs (AEDs) work by either decreasing neuronal excitation or increasing neuronal inhibition. Despite success with managing seizures, up to 1-in-3 patients with epilepsy do not find any relief with existing AEDs. A statistic that has not changed in over 50 years of drug development. With this in mind, the overarching goal of this dissertation is to explore the efficacy of targeting non-neuronal processes to treat epilepsy and broaden the search for new AED targets by further characterizing a unique mouse model of epilepsy. One such target studied in our lab is system xc- (SXC), a glutamate/cystine antiporter present on astrocytes, a non-neuronal cell that provides maintenance, support and protection for neurons. Investigations in tumor-associated epilepsy from our lab revealed that hyperactivity of SXC in tumor cells was directly related to the development of tumor-associated epilepsy. These studies also revealed that SXC inhibition using sulfasalazine (SAS), an FDA approved drug, can decrease seizure burden in a tumor mouse model. Therefore, the principal objective of this study is to further investigate the role of astrocytic SXC activity in the development of epilepsy and seizure generation. In this dissertation we show that SXC inhibition, using SAS, is able to decrease neuronal hyperactivity and decreases seizure burden in an astrogliosis-mediated epilepsy model.

Dedication

This journey in becoming a scientist has been a life-long endeavor and one of my most rewarding experiences. It is truly a privilege to explore and investigate the boundaries of our understanding of biology and life. This has also been one of my most demanding efforts and would never have been possible without the endless love and support of my family and friends.

To my parents – Gracias por ser el mejor ejemplo que un hijo podría tener y por siempre apoyar mis sueños, aun cuando ni yo los creía.

To my siblings – When some relationships began fading during my doctoral training, you doubled-down and made sure to be a daily presence in my life. This meant the world to me.

To Jenn –You never questioned my decision to pursue my dreams, even when it meant spending 4 years apart. This time apart has been more difficult than I ever imagined. I promise to make up for the lost time and cannot wait to get married when the pandemic ends.

Thank you all for your understanding of all the time and events I missed and for your support every step of the way. Pa'lante!

Acknowledgements

Dr. Campbell, none of this would have occurred without your encouragement and support early on in my training. You were always there to lend an ear, or a hug, regarding events in and outside of the lab. Thank you for your support, guidance and for pushing me to always reach higher.

Dr. Sontheimer, your passion towards science, research and education has always been palpable and one of the biggest reasons I wanted to join your lab within months of starting medical school. Thank you for providing an environment where I always felt encouraged to pursue my own original ideas and allowing me to forge my own scientific path. I would not be the scientist I am today without your support and guidance.

Dr. Tewari, thank you for never hesitating to drop what you were doing to help me troubleshoot, teach me a new technique or simply listen to my ideas and provide honest feedback. Your genuine love of conducting research is infectious and I strive to emulate that quality wherever my career takes me.

Dr. Olsen, Dr. Shah and all the lab members who have spent the time to teach me something new, listened to and provided feedback on my ramblings about my research and encouraged me to keep moving forward. Thank you!

Table of Contents

Chapter 1
Introduction

Introduction

Epilepsy affects approximately 2.2 million Americans, with around 150,000 new cases being diagnosed each year [8]. Although all epilepsies are characterized by spontaneous, recurrent seizures, this disease encompasses a diverse group of neurological disorders with distinct pathophysiology and a spectrum of severity. Broadly, the various causes of epilepsy can be grouped as genetic in nature, idiopathic or acquired. The International League Against Epilepsy defines epilepsy as a disease of the brain that induces at least two, unprovoked seizures more than 24 hours apart [9]. Seizures themselves are further classified into two broad groups: focal and generalized seizures. Focal seizures are characterized by their local nature, with neuronal ictal activity confined to one area of one cerebral hemisphere. The effects and manifestations of focal seizures correspond to the functions of the affected area of cerebral cortex [10]. Generalized seizures differ in their capacity to rapidly affect both cerebral hemispheres and can manifest as convulsive seizures, or grand mal seizures. One of the fundamental principles governing the pathophysiology of epilepsy is the imbalance between excitatory and inhibitory processes leading to neuronal hyperexcitability, hyperconnectivity and ultimately seizures.

Current options to treat epilepsy include surgical interventions and anti-epileptic drugs (AEDs). For a subset of patients with focal epilepsy, in which the seizure-onset zone has been clearly identified, resection of the affected area of the brain can improve seizure symptoms [11]. Dysfunctional voltage-gated sodium channels have also been implicated in the generation of generalized tonic-clonic seizures and partial seizures. AEDs that target sodium channels, such as carbamazepine and topiramate, aim to block the high-frequency repetitive firing patterns that can cause seizures [12]. AEDs, such as levetiracetam, target high voltage activated calcium channels to inhibit the aberrant release of neurotransmitters associated with seizures. However, despite

success with managing epileptic events, up to one in three patients with epilepsy experience drug resistant epilepsy[13,14]. Of note, a 1971 report on the clinical efficacy of AEDs found the efficacy at that time to be lower than 70-80% [15]. Thus, despite over 50 years of AED development, there continues to be a lack of effective therapeutics for around a third of epileptic patients.

These sobering statistics suggest that successful development of novel AEDs that are effective in medically refractory epilepsy may require the use of new models of epilepsy and broadening the search for new drug targets beyond the neuron. One such target extensively studied in our lab is the astrocytic membrane antiporter system xc- (SXC). The study of SXC began with Bannai and Kitamura who first isolated and characterized SXC in human fetal lung fibroblasts[16]. Early studies identified SXC as a sodium-independent, bidirectional antiporter of cystine and glutamate[17]. Importantly, under physiological conditions, astrocytic intracellular cystine is maintained at a low concentration due to rapid reduction of cystine to cysteine and intracellular glutamate is higher than extracellular concentrations [18]. Therefore, although SXC is bidirectional, physiological SXC activity results in extracellular release of glutamate and intracellular uptake of cystine in a 1:1 ratio. Investigations into the molecular identity of SXC revealed that it is

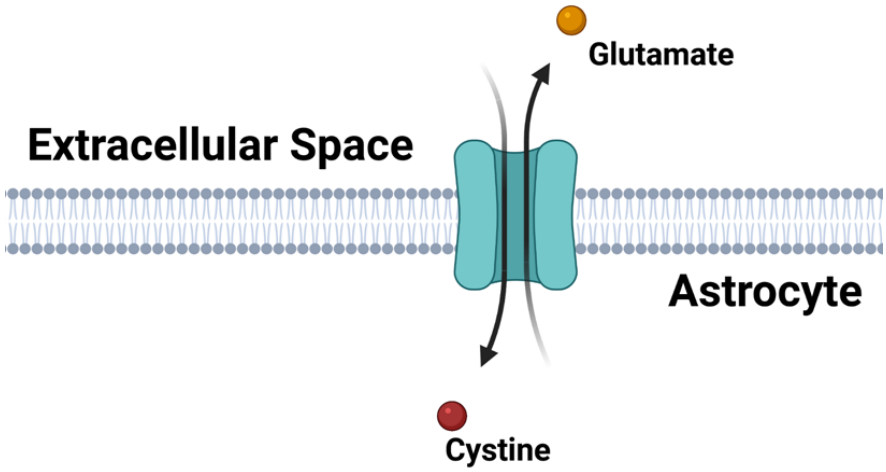

Figure 1: System xc- is a cystine/glutamate antiporter present on astrocytes in the CNS that leads to the extracellular release of glutamate in exchange for cystine uptake.

composed of a heavy chain unit 4F2hc (*SLC3A2)* and the specific light chain subunit xCT (*SLC7A11)* [19].

Early studies in our lab investigating the mechanisms of invasion and survival of aggressive glioblastomas found that gliomas have altered expression of astrocytic glutamate transporter GLT-1 and GLAST, leading to 100-fold lower levels of Na^+-dependent glutamate uptake compared to astrocytes[20]. Additionally, gliomas were found to highly express SXC which, combined with a reduction in glutamate uptake, was found to be a key mediator of elevated peri-tumoral glutamate concentrations which may contribute to neuronal hyperexcitability and tumor-associated epilepsy. Follow-up studies identified that release of extracellular glutamate via SXC in gliomas was likely a consequence of the need for highly metabolic gliomas to uptake cystine for the production of a critical antioxidant, glutathione [21,22]. Indeed, reducing the uptake of cystine in gliomas via inhibition of SXC led to depletion of glutathione and caspase-mediated apoptosis of gliomas in culture.

More recently our lab characterized how supraphysiological glutamate release by gliomas, via SXC, can induce epilepsy in mice implanted with human-derived gliomas [5,7]. This study confirmed increased expression of system xc- (SXC), a cystine/glutamate antiporter, in aggressive gliomas as a major contributor to elevated peritumoral glutamate *in vivo*. Glioma-induced epileptiform activity was shown to be susceptible to inhibition of SXC via sulfasalazine (SAS), an FDA-approved drug used to treat rheumatoid arthritis and inflammatory bowel disease. Importantly, SXC is not only expressed in gliomas but is also expressed in healthy brain parenchyma on astrocytes, supplying these cells with the antioxidant cystine in exchange for extracellular glutamate release[23].

Having characterized the contributions of SXC to tumor-associated epilepsy, the question of how SXC expression may affect other forms of acquired epilepsy remains. Investigations of SXC's role in the epileptogenesis of other forms of acquired epilepsy remains an area of active investigation. Notably, one study examining resected human epileptic tissue from patients with temporal lobe epilepsy found elevated SXC expression in diseased tissue compared to healthy [24]. Additionally, a recent study using the chemoconvulsant pilocarpine in rodents to induce epilepsy found elevated expression of SXC during the latent period of epileptogenesis[25].

In order to investigate the role of SXC in epileptogenesis and seizure generation we used a mouse model of epilepsy referred to as β1-integrin knockouts (B1KOs). Previously, our lab characterized the effects of knocking out astrocytic β1-integrin, a cell adhesion molecule, in mice[26]. Interestingly, tying a cre/lox mediated deletion of β-1 integrin to astrocytic GFAP expression leads to widespread, chronic astrogliosis in the brain, in the absence of gross abnormalities or neuronal loss. One outcome of chronic, widespread astrogliosis in β1-integrin knockouts (B1KO) is the development of spontaneous recurrent seizures by 4 weeks of age in mice[27]. This unique B1KO mouse model provides an excellent platform to isolate and study the relationship between astrogliosis and epilepsy without confounding factors present in chemoconvulsant animal models of acquired epilepsy, such as blood brain barrier loss, off-target peripheral effects and induction of neuronal excitotoxicity.

Taken together, the strong link between aberrant SXC expression on human gliomas and tumor-associated epilepsy along with evidence of SXC upregulation in other forms of epilepsy in humans and rodents, studying SXC as a therapeutic target for acquired epilepsy is warranted. As current treatments for epilepsy revolve around either decreasing excitatory neuronal mechanisms or enhancing inhibitory neuronal mechanisms, SXC provides a novel, non-neuronal treatment

modality for decreasing release of excitatory glutamate in the brain. The present dissertation aims to further elucidate the contribution of SXC in epilepsy in efforts to characterize a novel target that may offer relief to a third of epilepsy patients who do not respond to current AEDs.

The central hypothesis of this dissertation is that SXC-mediated glutamate release from astrocytes is involved in the pathology of epilepsy leading to neuronal hyperexcitability and seizure generation, and that lowering ambient extracellular glutamate, via SXC inhibition, can decrease seizure burden in epilepsy models. Towards this end, the following specific aims guided our investigations.

Aim 1: To determine if SXC inhibition can decrease hyperexcitability in chemically induced epilepsy models *ex vivo*. To evaluate whether SXC inhibition, via SAS, can decrease induced neuronal hyperexcitability, we used whole-cell patch clamp recordings and voltage-sensitive dye imaging on three distinct models of hyperexcitability in acute brain slices. Additionally, we tested whether co-administration of SAS with clinically prescribed AEDs would result in synergistic effects.

Aim 2: To determine whether chronic astrogliosis in B1KOs leads to higher SXC activity and whether SAS treatment decreases ambient glutamate and seizure burden *in vivo*. In order to evaluate whether there is increased SXC-activity and glutamate release in B1KOs we are using the glutamate-sensitive fluorescent reporter, iGluSnFR. Using iGluSnFR we can evaluate whether SAS application on acute brain slices from epileptic mice can decrease extracellular glutamate in response to SXC inhibition. To evaluate the *in vivo* efficacy of SAS in reducing seizure burden, we administered a one-week, twice daily SAS treatment paradigm and use 24/7 video-EEG to monitor and quantify behavioral seizures before and after treatment.

Aim 3: To identify additional epileptogenic mechanisms that result from chronic astrogliosis in beta-1 integrin knockouts (B1KO). To isolate the effects of astrogliosis in epileptogenesis we used B1KO mice, which are characterized by widespread, chronic astrogliosis and spontaneous seizures in the absence of induced physical or chemical injury. This unique model allows us to isolate the pro-epileptic effects of astrogliosis without confounding factors such as neuronal excitotoxicity, blood-brain barrier injury, or status epilepticus (SE). Using 24/7 video-EEG recordings, we will establish the typical behavioral seizure burden in this model, as well as utilize electrophysiology techniques to further characterize neuronal properties in this model. Additionally, we plan to investigate whether glutamate receptor expression patterns are altered with chronic astrogliosis using western blot.

Chapter 2

Literature Review

This chapter is adapted from a published review paper in Frontiers in Neurology

Dysregulation of Ambient Glutamate and Glutamate Receptors in Epilepsy: An Astrocytic Perspective

Alcoreza OB, Patel DC, Tewari BP and Sontheimer H (2021) Dysregulation of Ambient Glutamate and Glutamate Receptors in Epilepsy: An Astrocytic Perspective. Front. Neurol. 12:652159. doi: 10.3389/fneur.2021.652159

Abstract

Given the important functions that glutamate serves in excitatory neurotransmission, understanding the regulation of glutamate in physiological and pathological states is critical to devising novel therapies to treat epilepsy. Exclusive expression of pyruvate carboxylase and glutamine synthetase in astrocytes positions astrocytes as essential regulators of glutamate in the central nervous system (CNS). Additionally, astrocytes can significantly alter the volume of the extracellular space (ECS) in the CNS due to their expression of the bi-directional water channel, aquaporin-4, which are enriched at perivascular endfeet. Rapid ECS shrinkage has been observed following epileptiform activity and can inherently concentrate ions and neurotransmitters including glutamate. This review highlights our emerging knowledge on the various potential contributions of astrocytes to epilepsy, particularly supporting the notion that astrocytes may be involved in seizure initiation via failure of homeostatic responses that lead to increased ambient glutamate. We also review the mechanisms whereby ambient glutamate can influence neuronal excitability, including via generation of the glutamate receptor subunit GluN2B-mediated slow inward currents, as well as indirectly affect neuronal excitability via actions on metabotropic glutamate receptors that can potentiate GluN2B currents and influence neuronal glutamate release probabilities. Additionally, we discuss evidence for upregulation of System xc-, a cystine/glutamate antiporter expressed on astrocytes, in epileptic tissue and changes in expression patterns of glutamate receptors.

Introduction

The critical roles of astrocytes in supporting the healthy development and maintenance of a mature brain has been firmly established in the last few decades. It is well-appreciated that an imbalance between excitatory and inhibitory neurotransmission causes hyperexcitability in neuronal circuitry and underlies the processes of ictogenesis and epileptogenesis. Given the important functions that glutamate serves in excitatory neurotransmission, understanding the mechanisms regulating glutamatergic drive under physiological and pathological states provides critical insights into devising strategies to maintain glutamate homeostasis. Since 1-in-3 epilepsy patients are pharmacoresistant to currently available antiseizure drugs, that mainly target neuronal mechanisms[2,28], elucidating the astrocytic processes involved in seizure generation and epileptogenesis in detail may help identify new targets to treat intractable forms of epilepsy.

This review serves to highlight the emerging dynamic processes that astrocytes undergo in epilepsy, in support of the notion that astrocytes play a critical role in seizure generation via homeostatic responses such as the increase in ambient glutamate through a reduction in extracellular space (ECS) following activity-dependent astrocytic potassium uptake and buffering (Fig. 1-1). Importantly, we also review the mechanisms in which increased ambient glutamate can directly influence neuronal excitability, via generation of the glutamate receptor subunit GluN2B-mediated slow inward currents (SICs), as well as indirectly affect neuronal excitability via actions on metabotropic glutamate receptors (mGluRs) that can potentiate GluN2B currents, alter extracellular glutamatergic clearance, and influence neuronal glutamate release probabilities (Fig. 1-2). Additionally, evidence of upregulation of System x_c^- (SXC), a cystine/glutamate antiporter expressed on astrocytes, in epileptic tissue and changes in expression patterns of glutamate

receptors have provided insights in how astrocytic dysregulation can contribute to seizure generation and epileptogenesis (Fig. 1-3).

Glutamate synthesis, release, and reuptake

Before discussing the mechanisms whereby astrocytes regulate glutamatergic neurotransmission, it is important to understand the fundamental functions astrocytes play in CNS glutamate homeostasis. Glutamate or glutamic acid is a ubiquitous biological molecule serving multiple functions – mainly as an amino acid for protein synthesis, as a principal excitatory neurotransmitter in the mammalian CNS and as a source of energy[29]. The use of an abundant amino acid as a neurotransmitter poses a significant challenge in the regulation of available glutamate in the CNS, since excess extracellular glutamate is highly neurotoxic. The evolution of two remarkable features of the biological system –the blood-brain barrier (BBB) and the astrocytic specializations – has solved the problem of potential 'spillover' of peripheral glutamate into the CNS as a neurotransmitter. Interestingly, in both cases astrocytes are involved to the extent that glial dysfunctions can alter glutamate homeostasis and cause excitotoxicity and neuronal hyperexcitability.

The BBB is impermeable to glutamate[30], which is critical in preventing the flooding of the CNS by peripheral glutamate within the vasculature. However, this system also necessitates autonomous turnover of glutamate in the brain. The role of astrocytes in de novo synthesis of glutamate in the brain is well-established in literature[31].Astrocytes specializations, namely exclusive expression of pyruvate carboxylase and glutamine synthetase, allow them to serve critical functions in CNS glutamate homeostasis[32,33]. Since pyruvate carboxylase is essential for the synthesis of oxaloacetate that is subsequently utilized in the synthesis of α-ketoglutarate and glutamate, astrocytes are the only cell type in the brain capable of de novo synthesis of glutamate

by the oxidative metabolism of glucose. Although one study recently identified another source of glutamate in the brain where glutamate is synthesized by neurons from blood urocanic acid[34], more studies are required to validate it as well as to estimate the relative contribution of neurons in total glutamate synthesis in the brain. Glutamate is subsequently amidated by glutamine synthetase into glutamine, which enters the glutamate-glutamine cycle between astrocytes and neurons.

After release into the synaptic cleft, excessive glutamate must be cleared quickly to prevent neurotoxicity. There are no extracellular enzymes that can neutralize glutamate[35], however, astrocytes can rapidly clear glutamate from the synaptic clefts via astrocytic processes that completely enclose many glutamatergic synapses. These astrocytic processes also express highly efficient excitatory amino acid transporters[36] (EAATs) that take up 80% of extracellular glutamate in the CNS[31] (Fig. 1-1a). Once inside the astrocyte, it is estimated that ~85% of glutamate is converted into glutamine and returned to neurons, while the remaining ~15% is metabolized to α-ketoglutarate and further oxidized through the tricyclic acid cycle for energy production. This helps to cover the energy costs of glutamate handling as both pyruvate carboxylase and glutamine synthetase catalyze energy-dependent reactions[29]. Insights into the synthesis and regulation of glutamate in the CNS serve to highlight the role that astrocytes play in health and to set up the potential consequences of disrupting astrocytic glutamate homeostasis in the pathology of epilepsy.

Astrocytic regulation of ambient glutamate via volumetric shifts

Several recent reviews have emphasized the relationship between cerebral edema, astrocytic swelling, and epilepsy, due to a strong link between the volume reduction of the ECS hyperexcitability[37,38]. ECS is a narrow space between CNS cells that serves as a reservoir of water, ions and signaling molecules to maintain ionic and water homeostasis. Interestingly, ECS

reduction is one of the common mechanisms of generating hyperexcitability in several forms of epilepsies and astrocytes play key role in ECS volume regulation.

Astrocytes can significantly alter the volume of the CNS ECS due to their expression of the bi-directional water channel, aquaporin-4 (AQP4), which is enriched at perivascular endfeet[39]. Neuronal activity-dependent astrocytic swelling, following potassium uptake and buffering, is an important mediator in the reduction of ECS (Fig. 1-1b). Indeed, measurements of the ECS before and during bath application of picrotoxin, a $GABA_A$ receptor antagonist, to induce epileptiform activity revealed that brief epileptiform discharges rapidly decreased the median ECS width, measured as the width of interstitial space separating neural structures, by over 50%[40]. Rapid ECS shrinkage can inherently concentrate ions and neurotransmitters including glutamate, explaining elevated extracellular glutamate during seizures in epilepsy patients[41]. ECS shrinkage due to astrocyte swelling in hypoosmolar conditions has been shown to be sufficient in evoking large excitatory slow inward currents (SICs) in neurons[42]. Conversely, studies in AQP4-knockout animals have revealed that these mice have larger ECS, slower potassium kinetics and are more resistant to seizure generation using pentylenetetrazole (PTZ)[43-45], a $GABA_A$ receptor antagonist.

Another way astrocytes regulate water homeostasis and consequently ECS volume is the volume-regulated anion channel (VRAC), which are typically activated through hypotonicity-induced cell swelling[46,47]. VRAC belongs to the leucine-rich repeat-containing 8 (LRRC8) family of proteins[48,49] and consists of a heterogenous mix of LRRC8 proteins of which LRRC8A, also known as Swell1, is an essential subunit[50]. Upon astrocytic swelling, VRAC is activated and allows the release of chloride ions and other osmolytes, including glutamate (Fig. 1-1c). This in turn generates an osmotic gradient that drives water out of the astrocyte. Using astrocyte specific *Swell1* knockout mice and VRAC inhibitors, recent studies have identified that VRAC-mediated

glutamate release can modulate NMDAR-mediated tonic currents, as well as affect neuronal excitatory vesicle release probabilities[51,52].

These processes support the hypothesis that impairment in astrocyte functions may play a critical role in initial seizure generation by increasing physiologically relevant ambient glutamate through (1) a reduction of ECS, following astrocytic potassium uptake and buffering, (2) glutamate release through VRAC or (3) a dysregulated state combining both mechanisms.

Astrocytic regulation of ambient glutamate via SXC

Studies investigating the physiological role(s) of ambient glutamate (reviewed in Balázs Pál, 2018) have identified several diverse functions such as involvement in sleep-wakefulness cycles, synaptic plasticity and the ability to influence neuronal resting membrane potentials via induction of NMDAR-mediated inward currents. However, the processes that maintain and regulate levels of ambient glutamate continue to be elucidated[53]. Another important source of ambient, extracellular glutamate is via the sodium independent activity of the cystine/glutamate antiporter SXC. SXC is a covalently coupled heterodimeric protein complex comprised of the 4F2 heavy chain, *SLC3A2,* linked to the cystine/glutamate exchanger (xCT), *SLC7A11*. Notably, while xCT is abundantly expressed in cells throughout the body, examination of SXC knockout mice ($xCT^{-/-}$) mice revealed that in the CNS, xCT is exclusively expressed in astrocytes, and absent in neurons, oligodendrocytes, and microglia[23]. xCT plays a major role in the modulation of ambient extracellular glutamate as pharmacological inhibition of SXC, using (S)-4-carboxyphenylglycine (S-4-CPG), resulted in a 60% reduction in extrasynaptic glutamate in the nucleus accumbens[3]. Although S-4-CPG is known to inhibit type 1 mGluRs, this study found that use of the type 1 mGluR antagonist (RS)-1-aminoindan-1,5-dicarboxylic acid (AIDA) did not result in changes in ambient glutamate. This finding was confirmed recently using antisense xCT which similarly

decreased extracellular glutamate in the nucleus accumbens[4]. Additionally, $xCT^{-/-}$ mice have around 30% less hippocampal ambient glutamate[54].

In tumor-associated epilepsy, overexpression of SXC in glioblastomas and the corresponding increase in peritumoral glutamate levels have been directly associated with the development of seizures and poor patient survival[5-7]. These studies also found that inhibition of SXC via sulfasalazine (SAS), an FDA approved drug used to treat inflammatory bowel disease, reduced epileptiform activity and seizure frequency both *in-vitro* and *in-vivo* in glioblastoma models. In addition to tumor-associated epilepsy, resected human epileptic tissue from patients with temporal lobe epilepsy (TLE) also had an elevated expression of SXC[24] (Fig. 1-3a). We have also shown recently that SAS could significantly decrease the frequency and/or amplitude of evoked excitatory postsynaptic currents in multiple *in-vitro* models of hyperexcitability[55]. Furthermore, co-application of SAS with topiramate, an FDA-approved anti-seizure drug, further decreased epileptiform activity synergistically compared to topiramate alone.

The role of SXC in neuronal hyperactivity via ambient glutamate regulation is further supported by recent *in-vivo* studies on $xCT^{-/-}$ mice showing delayed epileptogenesis and reduced seizures in the self-sustained status epilepticus (SSSE) and pilocarpine induced status epilepticus models[56]. Additionally, this study found decreased micro- and astrogliosis in $xCT^{-/-}$mice after SSSE. In contrast, wildtype mice that underwent pilocarpine-induced status epilepticus had significantly increased xCT expression during latent phase of epileptogenesis. Using another strain of SXC knockout mice, which have a spontaneous deletion in the xCT gene in subtle gray mice ($xCT^{sut/sut}$), it was found that $xCT^{sut/sut}$ mice were significantly resistant to epileptic kindling compared to wildtype mice. Additionally, western blot analysis of plasma membrane proteins

found that cortical, but not hippocampal, surface GluA1 expression was significantly decreased in $xCT^{sut/sut}$ mice[57].

In contrast to the above studies that show a pivotal role of SXC in hyperexcitability, a recent study using the Theiler's Murine Encephalomyelitis Virus (TMEV) model of viral-induced epilepsy found that $xCT^{-/-}$ mice were not protected against this form of epilepsy and had similar number and severity of behavioral seizures[58]. The lack of difference in TMEV-induced seizures between $xCT^{-/-}$ and WT mice can be possibly explained by the fact that the proinflammatory cytokines, tumor necrosis factor-α and interleukin-6, are known as the major drivers of hyperexcitability and seizures in this epilepsy model[59,60]. Taken together, these above cited studies establish SXC as a potential astrocytic drug target. Clearly astrocytes have the capabilities to modulate ambient extracellular glutamate, yet whether astrocytic SXC exerts a direct, pro-epileptic effect by modulating ambient glutamate in acquired epilepsies requires further study.

Mechanisms of astrocyte-derived glutamate contributing to neuronal hyperexcitability

So far, we have discussed that astrocytes not only prevent excitotoxic glutamate accumulation in the ECS, but also serve as a source of extracellular glutamate under specific conditions. However, important questions remain. How might astroglial glutamate contribute to neuronal activity, and is it sufficient to trigger neuronal hyperactivity? Additionally, how might different types of glutamate receptors at tripartite synapses and extrasynaptic spaces respond to fluctuations in ambient glutamate?

The notion of glial-neuronal crosstalk via gliotransmission has been extensively studied in the last two decades. Regardless of the mechanisms, a wealth of evidence has demonstrated that astrocytes can sense neuronal activity and respond through the release of gliotransmitters including

ATP, D-serine, and glutamate[61,62]. Research into the origin and consequences of neuronal SICs revealed that these currents are generated via astrocyte-derived glutamate acting on extrasynaptic GluN2B subunit-containing N-methyl D-aspartate type of glutamate receptors[63,64] (NMDARs) (Fig. 1-2a). Extrasynaptic NMDARs are thought to have increased GluN2B-containing heterodimers, suggesting a spatially specific function. Indeed, GluN2B-containing NMDARs have a higher affinity for glutamate compared to GluN2A-containing NMDARs[65], which may facilitate sensing glutamate in the extrasynaptic space that has far lower extracellular glutamate compared to an active synapse.

SICs can be synchronized in multiple neurons over 100 microns apart in the hippocampus, raising the possibility of astrocytic synchronization of neuronal hyperactivity in epilepsy. Interestingly, blockade of glutamate uptake and exocytotic glutamate release increased the frequency and amplitude of these NMDAR-mediated SICs, suggesting that increases in ambient glutamate could play a physiologically relevant role[64]. A study investigating the actions of extrasynaptic glutamate determined that SXC-mediated glutamate release preferentially activates extrasynaptic GluN2B-containing NMDARs[66]. Similarly, another study determined that the glutamate responsible for generating SICs occur independently from exocytotic Ca^{2+}-dependent glutamate release[67]. Notably, a paper examining the sensitivities of glutamate receptors to glutamate predicted the percentage of glutamate receptors that would remain activated at increasing levels of ambient extracellular glutamate[68]. This paper succinctly demonstrates that NMDARs and mGluRs would be preferentially activated by small, local fluctuations in astrocytic glutamate release as they are activated by glutamate concentrations around 1–30μM, while α-amino-3-hydroxy-5-methyl-4-isoxazolepropionic acid type of glutamate receptors (AMPARs) are only activated in the presence of 100–3000μM of glutamate. Therefore, it is evident that astrocytes

possess the molecular machinery necessary to significantly alter the concentration of extrasynaptic ambient glutamate, which can act on NMDARs to induce neuronal SICs that can contribute to hyperexcitability.

Metabotropic glutamate receptors and epilepsy

Metabotropic glutamate receptors (mGluRs), which are coupled to G protein-coupled pathways and G protein-independent pathways, are another class of glutamatergic receptors whose dysregulation have been implicated in the pathology of epilepsy. Unlike ionotropic glutamate receptors, mGluR activation can trigger long-term changes in cellular signaling by regulating the expressions of various homeostatic and glutamatergic proteins in neurons and glial cells[69]. Currently, eight mGluR subtypes have been described that fit into 3 subgroups[70,71]. Group 1 mGluRs consists of mGluR1 and mGluR5 and are coupled to $G\alpha_{q/11}$, which stimulates the release of Ca^{2+} from intracellular stores upon activation. Group 1 mGluRs are thought to be distributed primarily on post-synaptic neurons, in the perisynaptic zone[72,73]. Using the kainic acid (KA) rat model of TLE, one study has reported upregulation of neuronal mGluR1 in rodent hippocampi, in addition to, mGluR1 upregulation in human TLE tissue[74]. Importantly, neuronal mGluR1 activation was shown to potentiate NMDAR-mediated currents via a mechanism involving Ca^{2+}, calmodulin and Src-dependent activation of proline-rich tyrosine kinase leading to tyrosine phosphorylation of NMDAR subunits GluN2A/B[75] (Fig. 1-2b). A study investigating the efficacy of mGluR1 inhibition in epilepsy found that mGluR1 inhibition decreased PTZ-induced seizures, and this effect could be prevented by adding mGluR1 agonists[76].

mGluR5 is also expressed on cortical and hippocampal astrocytes, primarily during development[77], however, the reappearance of mGluR5 expression has been observed in astrocytes of specific epilepsy animal models, and human epileptic tissue[78-80]. Intriguingly, mice with

persistent astrocytic mGluR5 expression during the latent period reliably went on to develop epilepsy, whereas mice with only transient mGluR5 expression did not[78] (Fig. 1-3b). Additionally, epileptic mice with astrocytic mGluR5 knocked out displayed lowered glutamate uptake kinetics during high-frequency stimulation compared to epileptic wildtype mice. Downstream effects of astrocytic mGluR5 activation include increased Ca^{2+}-dependent, GluN2B-subunit containing NMDAR-mediated neuronal currents[80]. *In vivo* loading of BAPTA-AM, a Ca^{2+}chelator, selectively into astrocytes was found to be neuroprotective and significantly reduced the amount of Fluoro-Jade B labeling of dying neurons. Together, these findings suggest that reappearance of astrocytic mGluR5 may be a useful biomarker for active epileptogenesis, as well as a contributor to epileptogenesis by potentiating GluN2B-mediated inward neuronal currents.

Group 2 mGluRs consist of mGluR2 and mGluR3, while Group 3 mGluRs consist of mGluR4, mGluR6, mGluR7 and mGluR8. Both Group 2 and Group 3 inhibit adenylyl cyclase activity through $G\alpha_i$ activation and are thought to be largely distributed on pre-synaptic neurons, where they act to inhibit glutamate and GABA release[81,82]. Additionally, mGluR3 has been reported to be expressed on post-synaptic neurons and astrocytes[83-85]. Using the pilocarpine TLE animal model, studies have shown that neuronal mGluR2/3 expression in the hippocampus[86,87] and cortex[88] are decreased in epilepsy. Additionally, epileptic tissue from patients with TLE also have decreased mGluR2/3 expression[89] (Fig. 1-2c). As pre-synaptic Group 2 mGluRs are thought to inhibit glutamate release, down-regulation of these receptors could promote glutamate release and neuronal hyperexcitability. Indeed, studies using Group 2 mGluR agonists have been shown to be neuroprotective in the models of absence epilepsy and the epilepsy models induced through amygdala kindling[76,90]. Conversely, Group 2 mGluR antagonists were shown to be pro-epileptic in an absence epilepsy model[91]. Notably, these researchers also found that a mGluR1

potentiator,9H-xanthene-9-carboxylic acid(4-trifluoromethyl-oxazol-2-yl)amide (SYN119), played a protective role against spike and wave discharges in a rat model of absence epilepsy[92].

One study investigating the localization and changes in mGluR3 and mGluR5 expression after hippocampal injury via KA-induced seizures found that mGluR3 mRNA was exclusively upregulated in astrocytes and oligodendrocytes (Fig. 1-3c). Additionally, GFAP-positive astrocytes were found to be persistently upregulated from 2 days to 12 weeks post hippocampal injury[93]. Although mGluR5 mRNA was not found to be upregulated in astrocytes, other studies have reported upregulated mGluR5 protein levels in animal models of epilepsy[94,95]. To understand how changes in astrocytic mGluR3 or mGluR5 activity may affect seizure generation, one study looked at the effects of adding Group I and Group II modulators to cultured astrocytes[96]. This paper found that astrocytic Group 1 mGluR activation, via the use of (S)-3,5-dihydroxyphenylglycine ((S)-3,5-DHPG), led to decreased expression of glutamate transporters (GLAST and GLT-1), and that this effect could be antagonized using a selective mGluR5 antagonist, MPEP. Conversely, astrocytic Group II mGluR activation, using DCG-IV, resulted in upregulation of GLAST and GLT-1 expression, and this effect could be abolished using the Group II antagonist EGLU. As mGluR2 has not been found to be expressed by astrocytes, the authors concluded that the effects of Group II modulation in these experiments was attributable to astrocytic mGluR3 activity.

Questions remain and more work certainly needs to be done to further elucidate the role of mGluRs in epilepsy, however, it appears evident that mGluR expression and activity are significantly altered both in animal models and human epileptic tissue in ways that contribute to hyperexcitability and epileptogenesis. Although ionotropic and metabotropic glutamate receptors

differ fundamentally in their structure and downstream effectors, NMDARs and mGluRs share the ability to sense changes in ambient glutamate and potentiate neuronal inward currents.

Discussion

Supporting the notion that astrocytes are critically involved in the initiation of seizures through dysregulation of ambient glutamate, a recent *in silico* study found that increased ambient glutamate, either through increased astrocytic glutamate release or decreased uptake, was sufficient to initiate synchronous epileptiform-like discharges from neurons[97]. Additionally, the use of transparent zebrafish combined with two-photon calcium imaging and local field potential recordings allowed investigators to monitor the activity and connectivity of thousands of neurons and glia revealing new insights into the role glia may play in seizure generation[98]. Using PTZ, a GABAaR antagonist, to initiate seizures investigators found that pre-ictal neuronal activity did not significantly increase in synchrony, however, radial glia exhibited a significant increase in synchrony during the pre-ictal period followed by neuronal bursts. These findings support the idea that the local, pro-epileptic glial responses presented throughout this review can culminate in network-level events that can ultimately lead to neuronal hyperexcitability synchronization and seizure initiation.

Knowing that current anti-seizure therapeutics are ineffective for 1-in-3 people living with epilepsy[2,28], elucidating the astrocytic processes involved in epileptogenesis may help identify new therapeutic targets that offer relief to patients with intractable epilepsy. Table 1 summarizes current FDA-approved and investigational pharmacotherapies targeting glutamate signaling for epilepsy. In summary, astrocytes exclusively possess the enzymatic activity to generate *de novo* glutamate in the CNS, as well as the molecular machinery to determine ambient glutamate through (1) a reduction of ECS, (2) glutamate release through SXC or VRAC or (3) a dysregulated state

combining these mechanisms. Importantly, ambient glutamate can directly influence neuronal excitability, via generation of GluN2B-mediated SICs, as well as indirectly affect neuronal excitability via actions on mGluRs that can potentiate GluN2B-mediated currents, alter extracellular glutamatergic clearance, and influence neuronal glutamate release probabilities. Although inherent challenges exist in ubiquitously targeting glutamatergic mechanisms in the CNS, it appears clear that astrocytes are uniquely positioned to act as a master regulator of glutamate in health, and when dysregulated, can mediate pro-epileptic changes that warrant further investigation in hopes of unveiling novel therapeutic targets.

Figure 1:

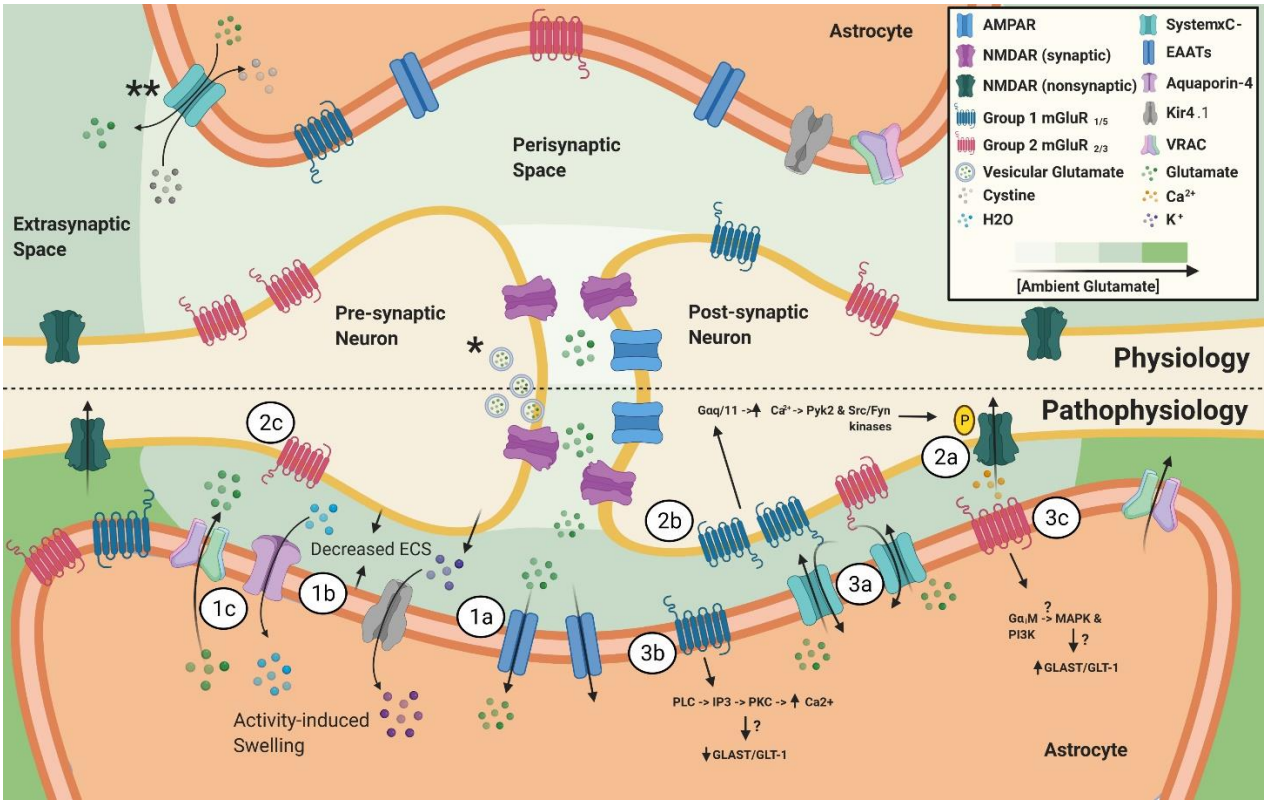

* Vesicular glutamate release during action potentials is the primary source of synaptic glutamate. ** SXC, primarily expressed on astrocytes, is a major source of ambient, extrasynaptic glutamate. Ambient glutamate concentration around the synapse, after EAAT activity, follows a gradient with the lowest level in the synaptic cleft to the highest in the extrasynaptic compartment. **1. Astrocyte homeostatic responses to increased activity from hyperexcitable neurons.** 1a: Increased vesicular glutamate release from hyperexcitable neurons leads to increased astrocytic EAAT activity. 1b: Elevated neuronal activity also causes release of K^+ , in attempts to maintain homeostatic neuronal resting membrane potential. Next, astrocytic buffering of extracellular K^+ through elevated Kir4.1 activity, which is accompanied by increased H20 uptake through aquaporin-4, ultimately results in activity-induced astrocytic swelling and reduction in ECS. 1c: Astrocytic swelling leads to activation of VRAC and release

of glutamate and other gliotransmitters into the ECS. **2. Pathophysiological effects of increased activity and changes in expression of neuronal extrasynaptic glutamate receptors.** 2a: Activation of N2B-containing NMDARs leads to the generation of slow, depolarizing currents. 2b: Elevated expression and activity of group 1 mGluRs in epilepsy has been linked to increased NMDAR-mediated currents via a mechanism involving Ca^{2+}-calmodulin dependent tyrosine phosphorylation of NMDAR subunits NR2A/B. 2c: Presynaptic group 2 mGluRs have been shown to inhibit glutamate and GABA release. Tissue from epileptic patients and animal models have revealed decreased $mGluR_{2/3}$ expression, which can contribute to a pro-epileptic brain state. 3. **Changes in astrocytic glutamatergic protein expression in epilepsy.** 3a: SXC expression has been found to be elevated in human epileptic tissue, as well as various epilepsy animal models. SXC activity leads to the release of glutamate from astrocytes. 3b: Animal models of epilepsy have revealed that persistent upregulation of astrocytic $mGluR_5$ was a reliable indicator of epileptogenesis. $mGluR_5$ activation leads to altered GLAST/GLT-1 expression and induces NR2B-dependent NMDAR mediated neuronal currents. 3c: Upregulation of $mGluR_3$ has been reported in epilepsy animal models and experimental activation of group 2 mGluRs in cultured astrocytes was shown to upregulate GLAST/GLT-1 expression, suggesting that a balance of group 1 and group 2 mGluRs on astrocytes is important in maintaining homeostatic extracellular glutamate.

Table 1 - Pharmacotherapies targeting glutamate signaling for epilepsy

Drug	Brief mode of action	Effects on glutamatergic system	Effects on seizures	Developmental Stage	Reference
Perampanel	Noncompetitive selective AMPAR antagonist	↓ AMPAR-mediated fast excitatory neurotransmission	↓ focal and generalized tonic-clonic seizures	FDA-approved in 2012	99
Topiramate	AMPAR/KAR inhibitor; multiple other mechanisms	↓ excitatory neurotransmission	↓ focal and generalized convulsive seizures	FDA-approved in 1995	100
Felbamate	NMDAR inhibitor; multiple other mechanisms	↓ excitatory neurotransmission	↓ focal and generalized convulsive seizures	FDA-approved in 1993	101
Ketamine	NMDAR antagonist	↓ NMDAR-mediated excitatory neurotransmission; potentially neuroprotective	efficacious against refractory status epilepticus	Under clinical trial	102
Gabapentinoids (Gabapentin, Pregabalin)	Blocker of α2δ subunit of voltage-gated Ca2+ channel	↓ release of glutamate	↓ focal seizures (gabapentin, pregabalin)	FDA-approved (Gabapentin, 1993; Pregabalin, 2004)	103
		↓ excitatory synaptogenesis	↓ generalized convulsive seizures (gabapentin)		100
		inhibits surface trafficking and synaptic targeting of NMDAR			
Levetiracetam	Synaptic vesicle glycoprotein 2A (SV2A) modulator	↓ release of glutamate, ↑ synaptic depression	↓ focal and generalized tonic-clonic seizures; potentially antiepileptogenic	FDA-approved in 2000	104,105
Brivaracetam	SV2A modulator (more selective than levetiracetam)	↓ release of glutamate, ↑ synaptic depression	↓ focal and generalized tonic-clonic seizures	FDA-approved in 2016	104,105
17AAG	HSP90β inhibitor	inhibits internalization and proteosomal	↓ seizures in intrahippocampal	Investigational	106

		degradation of GLT-1	kainate model of epilepsy		
		↑ glutamate clearance from ECS			
Ceftriaxone	GLT-1 transcriptional activator	↑ glutamate clearance from ECS	↓ frequency and duration of post-traumatic seizures	Investigational	[107]
		↓ excitotoxic loss of inhibitory interneurons			[108]
		↑ intracellular glutathione and ↓ oxidative stress			[109]
Sulfasalazine	System X_c^- transporter inhibitor	↓ extracellular level of glutamate	↓ seizures in a murine model of tumor-associated epilepsy	Investigational	[5]
		↑ intracellular glutathione and ↓ oxidative stress			
LY367385, LY339840	mGluR1 antagonist	↓ excitatory neurotransmission	potent anticonvulsant activity in animal models of seizures	Investigational	[110,111]
		↓ glutamate release from presynaptic terminals and perisynaptic astrocytic processes			[112]
MPEP	mGluR5 negative allosteric modulator	↓ excitatory neurotransmission	potent anticonvulsant activity in animal models of seizures	Investigational	[113,114]
		↓ glutamate release from presynaptic terminals and perisynaptic astrocytic processes			[112]
S-4C3HPG	mGluR1 antagonist, mGluR2 agonist	↓ glutamate release and neurotransmission	protects against audiogenic seizures in DBA/2 mice	Investigational	[115]
			suppresses PTZ and DMCM-induced seizures		[116]

2R,4R-APDC	Group 2 mGluR agonist	↓ glutamate release and neurotransmission	enhance seizure threshold in a rat model of amygdala kindling	Investigational	[117]
DCG-IV	Group 2 mGluR agonist	↓ glutamate release and neurotransmission	↓ kainate and amygdala kindling-induced seizures	Investigational	[117,118]
JNJ-42153605, JNJ-40411813, JNJ-46356479	mGluR2 positive allosteric modulator	↓ glutamate release and neurotransmission	anticonvulsant effect in the mouse 6-Hz and corneal kindling models	Investigational	[119,120]
			enhances antiseizure efficacy of levetiracetam		
LY404039	Group 2 mGluR agonist	↓ glutamate release and neurotransmission	anticonvulsant effect in a model of 6 Hz psychomotor seizures	Investigational	[119]
			enhances antiseizure efficacy of levetiracetam		

17AAG – 17-allylamino-17-demethoxygeldanamycin
HSP90β – Heat shock protein 90β
MPEP – 2-methyl-6-phenylethynyl-pyridine
S-4C3HPG – S-4-carboxy-3-hydroxyphenylglycine
PTZ – pentylenetetrazol
DMCM – methyl-6,7-dimethoxy-4-ethyl-beta-carboline-3-carboxylate
2R,4R-APDC – 2R,4R-1-aminocyclopentane dicarboxylic acid
DCG-IV – 2S,2'R,3'R-2-(2',3'-dicarboxycyclopropyl)glycine

Chapter 3

This chapter is adapted from a published manuscript in Epilepsia

Sulfasalazine Decreases Mouse Cortical Hyperexcitability

Alcoreza O, Tewari BP, Bouslog A, Savoia A, Sontheimer H, Campbell SL. Sulfasalazine decreases mouse cortical hyperexcitability. Epilepsia. 2019 Jul;60(7):1365-1377. doi: 10.1111/epi.16073. Epub 2019 Jun 18. PMID: 31211419; PMCID: PMC6771750.

Abstract

Objective: Currently prescribed antiepileptic drugs (AEDs) are ineffective in treating approximately 30% of epilepsy patients. Sulfasalazine (SAS) is an FDA approved drug for the treatment of Crohns disease that has been shown to inhibit the cystine/glutamate antiporter system xc- (SXC) and decrease tumor-associated seizures. This study evaluates the effect of SAS on distinct pharmacologically-induced network excitability and determines whether it can further decrease hyperexcitability when administered with currently prescribed AEDs.

Methods: Using in vitro cortical mouse brain slices, whole-cell patch-clamp recordings were made from layer 2/3 pyramidal neurons. Epileptiform activity was induced with bicuculline (bic), 4-aminopyridine (4-AP) and magnesium free (Mg2+-free) solution to determine the effect of SAS on epileptiform events. In addition, voltage-sensitive dye (VSD) recordings were performed to characterize the effect of SAS on the spatiotemporal spread of hyperexcitable network activity and compared to currently prescribed AEDs.

Results: SAS decreased evoked excitatory postsynaptic currents (eEPSCs) and increased the decay kinetics of evoked inhibitory postsynaptic currents (eIPSCs) in layer 2/3 pyramidal neurons. While application of SAS to bicuculline and Mg2+-free-induced epileptiform activity caused a decrease in the duration of epileptiform events, SAS completely blocked 4-AP-induced epileptiform events. In VSD recordings, SAS decreased VSD optical signals induced by 4-AP. Co-application of SAS with the AED topiramate (TPM) caused a significantly further decrease in the spatiotemporal spread of VSD optical signals.

Significance: Taken together this study provides evidence that inhibition of SXC by SAS can decrease network hyperexcitability induced by three distinct pharmacological agents in the

superficial layers of the cortex. Also, SAS provided additional suppression of 4-AP-induced network activity when administered with the currently prescribed AED TPM. These findings may serve as the foundation to assess the potential for SAS or other compounds that selectively target SXC as an adjuvant treatment for epilepsy.

1 Introduction

Epilepsy is the most chronic and progressive neurological disorder and affects an estimated 50 million individuals worldwide. 1-in-26 people will develop epilepsy within their lifetime[1]. Despite the development of numerous antiepileptic drugs (AEDs) over the past 20 years, which provide more options for clinicians and patients, current treatment regimens fail in up to 30% of patients[2,28]. This increase in treatment options has prompted an interest in the efficacy of combination AED therapy to utilize drugs with differing pharmacological properties.

As most AEDs were generated by targeting neuronal inhibitory and excitatory mechanisms, the contribution of glial cells to the pathophysiology of epilepsy is increasingly being explored[121]. Further it is widely accepted that astrocyte dysfunction is a crucial player in epilepsy[122,123]. One potential new target is SXC, a glutamate/cystine antiporter primarily expressed on astrocytes, which has been implicated in several psychological and neurological disorders[124]. SXC knockout mice were found to be less susceptible to seizure induction compared to wild types, and the increased threshold was attributed to a 40% reduction in extracellular hippocampal glutamate levels[54]. In addition to its role in glutamatergic signaling, SXC plays a major role in the cystine/cysteine cycle. SXC mediates the uptake of cystine into astrocytes, which is then reduced to cysteine and released to be taken up by neurons as the rate-limiting precursor for synthesis of glutathione, a critical antioxidant[125]. The role of SXC, at the crossroads between excitatory signaling and managing oxidative stress, makes it an intriguing target for the treatment and prevention of acquired epilepsy.

Sulfasalazine (SAS) is an FDA-approved drug for rheumatoid arthritis and inflammatory bowel disease. We previously showed that SAS decreased tumor-associated seizures in a mouse model of glioma[5]. In this model glutamate release by glioblastoma cells, via SXC, induced peri-

tumoral neuronal excitotoxicity and contributed to tumor-associated epilepsy. A subsequent pilot clinical study found that acute SAS treatment reduced extracellular glutamate levels, by inhibiting SXC in glioma patients[7].

As the mechanisms of seizure development involve a complex interplay of aberrant neuronal network activity[126], various *in vitro* pharmacological models of hyperexcitability have been utilized to assess novel AEDs. Use of Mg^{2+}-free ACSF for *in vitro* electrophysiology removes the magnesium block from NMDA receptors, resulting in neuronal hyperexcitability, as previously described[127]. As a $GABA_A$ receptor antagonist, bicuculline (bic) simulates neuronal hyperexcitability by decreasing inhibition while 4-aminopyridine (4-AP) reduces neuronal K^+ repolarization. While all chemically-induced models are valuable for studying seizure mechanisms, variations in models can affect end results.

In this study, we used whole-cell patch clamp recordings of layer II/III pyramidal cells and voltage-sensitive dye (VSD) imaging to evaluate SAS's effect on three chemically-induced *in vitro* models of hyperexcitability. Our findings indicate that SAS has significant effects on decreasing hyperexcitability at the cellular and network levels in all the pharmacologically-induced models we tested. We also provide evidence that concomitant use of topiramate (TPM), an AED used to treat generalized-onset tonic-clonic seizures[128], and SAS results in additional anti-epileptic effects, compared to the use of TPM alone. Based on these findings, we believe that further investigation of SXC and its modulation by SAS may allow us to unravel some of the complex, extra-synaptic processes associated with the pathogenesis of acquired epilepsy, which could lead to novel therapeutics for patients with intractable epilepsy.

2 Materials and Methods

2.1 Animals

Animals were housed and handled according to the guidelines of the National Institutes of Health Committee on Laboratory Animal Resources. Prior approval of the University of Alabama at Birmingham Institutional Animal Care and Use Committee was obtained for all experimental protocols. All efforts were made to minimize pain. Experiments were performed using 4 to 6-week-old C57Bl6 mice.

2.2 Slice Preparation

Mice were anesthetized and decapitated and their brains were quickly removed and immersed in ice-cold cutting solution containing (in mM): 135 N-methyl-D-glucamine (NMDG), 1.5 KCl, 1.5 KH2PO4, 23 mM choline bicarbonate, 25 D-glucose, 0.5 mM CaCl2, 3.5 MgSO4 (Sigma-Aldrich). Coronal brain slices (300 μm) were made and recovered for 40-60 min in oxygenated recording solution in mM: 125 NaCl, 3 KCl, 1.25 NaH2PO4, 25 NaHCO3, 2 CaCl2, 1.3 MgSO4, 25 D-glucose at 32 ℃ and maintained at room temperature before recordings.

2.3 Whole-cell recordings

Individual brain slices were transferred to a recording chamber and continuously perfused (4ml/min) with oxygenated recording solution. Whole-cell recordings were conducted using borosilicate glass capillaries (KG-33 glass, Garner Glass) and filled with internal solution containing (in mM): 134 K-gluconate, 1 KCl, 10 HEPES, 2 mg-ATP; 0.2 Na-GTP and 0.5 ethylene glycol tetraacetic acid (EGTA). The pH was set to 7.24 with KOH, and the osmolality was measured (~290 mOsm/kg). All recordings were performed at 32 ± 1°C. Individual cells were visualized using a Zeiss Axioscope (Carl Zeiss, Thornwood, NY) microscope equipped with

Nomarski optics with a 40X water immersion objective lens. Tight seals were made using electrodes with a 3–5-MΩ open-tip resistance. Signals were acquired from layer II/III pyramidal cells with an Axopatch 1B amplifier (Molecular Devices), controlled by Clampex 10 software via a Digidata 1440 interface (Molecular Devices). To isolate GABAergic inhibitory postsynaptic currents (IPSCs), slices were perfused with ACSF containing 20 µM 6-cyano-7-nitroquinoxaline-2,3-dione (CNQX, Fisher), and 50 µM D-(-)-2-amino-5-phosphonovaleric acid (APV, Sigma) and recorded at -70 mV. Excitatory postsynaptic currents (EPSCs) were obtained in the presence of bic (10 µM; Sigma-Aldrich, St. Louis, MO) to block $GABA_A$ receptors. NMDA receptor-mediated currents were isolated in the presence of bic and CNQX and recorded at -40 mV. AMPA receptor-mediated EPSCs were isolated at a holding potential of -70 mV in the presence of bic and APV. A twisted pair of Formvar-insulated nichrome wires was positioned in deeper cortical layer IV, to evoke synaptic responses. Stimulation intensity was 20 -200 µA pulses for 50 µs at 0.05 Hz. Representative traces are averages of 10 consecutive responses. Responses were filtered at 5 kHz, digitized at 10-20 kHz, and analyzed off-line with Clampfit 10.0 software.

2.4 Voltage-sensitive dye imaging

Optical recordings were conducted using the voltage-sensitive fluorescent dye N-[3-(triethylammonium)propyl]-4-[4-(p-diethylaminophenyl)butadienyl]pyridinium dibromide (RH 414). Individual slices were incubated with 30 µM RH414 for at least 60 min, then slices were transferred to a recording chamber on an Axiovert 135 TV (Zeiss) microscope. The microscope was equipped with NeuroPlex 464-element photodiode array (Red Shirt Imaging, Fairfield, CT), as previously described[129]. A bipolar stimulating electrode placed in cortical layer IV was used to evoke activity, with stimulation intensities from 20 to 100 µA in amplitude and 100 µs in duration. Changes in fluorescence were detected by a hexagonal photodiode array containing 464 diodes

(Neuroplex, Red Shirt Imaging, Fairfield, CT). Excitation of the dye was achieved with a stabilized power supply (Hewlett-Packard, Palo Alto, CA), a 100-W halogen lamp, and a 535 ± 40 nm filter. Fluorescent measurements were obtained by normalizing the resting light intensity for each diode. Dye bleaching corrections was done by acquiring measurements in the absence of stimulation. Optical signals are represented as change in fluorescence with stimulation divided by resting fluorescence (ΔF/F). The responses to 3 consecutive stimulations were averaged. RH 414 responds to membrane depolarization with a decrease in the fluorescence intensity. Optical signals were amplified and stored on a computer for later analysis. Pseudocolor images were generated to visualize spatiotemporal spread of activity.

2.5 Drug application

All drugs were bath applied. SAS (Fisher) was dissolved in 0.1N NaOH solution to create a 10 mM stock solution and used at 250 µM. 4-AP (50 µM), TPM (50 µM), and levetiracetam (LEV) (100 µM) were purchased from Sigma Aldrich. S-4CPG (100 µM) was purchased from Tocris. For VSD recordings, slices were exposed to bic (10 µM), 4AP and Mg^{2+}free for at least 45 mins before recordings. TPM, LEV and SAS were incubated for 30 mins before recordings. In co-application experiments, SAS was added in the presence of LEV and TPM.

2.6 Statistics

Changes in evoked E/IPSCs were analyzed using Clampfit Software 10.0 (Molecular Devices, Union City, CA). Paired Student's t test were used for means comparisons among the number and duration of epileptiform events, and amplitude of currents in whole-cell recordings. A 2-way repeated measures ANOVA (varying conditions as between-subject factors and stimulation intensity as a repeated measure) and Tukey’s post hoc tests were used for statistical

comparison of VSD recordings. Statistics were generated and graphed using Origin 7.5 Pro software (Origin), significance set at $P < 0.05$. Figures display box-and-whisker plots (minimum to maximum, median line) or histograms (mean ± standard error of mean). Values in the text report mean ± standard deviation.

3 Results

3.1 Sulfasalazine decreases evoked excitatory postsynaptic currents (eEPSCs)

We first examined the effects of SAS on eEPSCs using whole-cell patch-clamp recordings of layer II/III pyramidal cells in the prefrontal cortex. Synaptic responses were elicited via intracortical stimulations 150 - 200 µm below the recording pipette. We isolated eEPSCs by recording in the presence of bic to block $GABA_A$ receptor mediated currents and cells were held at -70 mV. Following baseline recordings, infusion of SAS for 10 minutes reversibly decreased eEPSC amplitude (control: 289.43 ± 130.20 -pA; SAS: 172.41 ± 91.61 -pA, $p = 0.001$, Fig. 1A, B).

3.2 Sulfasalazine decreases evoked inhibitory postsynaptic currents (eIPSCs)

To investigate the effects of SAS on eIPSCs, we obtained whole-cell patch-clamp recordings in the presence of APV (20 µM) and CNQX (10 µM) to block ionotropic glutamate receptors. We found that bath application of SAS significantly decreased the eIPSC amplitude (control: 291.92 ± 139.82 pA; SAS: 98.40 ± 83.49 pA, $p = 0.003$, Fig. 1C, D). When the current decay of eIPSC was fit by a sum of two exponentials, we observed a significant increase in the decay kinetics of the τ_{slow} response in the presence of SAS (control τ_{slow}: 75.31 ± 48.19 ms; SAS τ_{slow}: 241.30 ± 124.30 ms, $p = 0.03$, Fig. 1 E, F). The τ_{fast} response was not significantly altered by SAS (control τ_{fast}: 10.18 ± 9.84; SAS τ_{fast}: 23.96 ± 32.17 ms, $p = 0.42$, Fig 1E, F). These effects

appeared to be reversible as eIPSC amplitude partially recovered during a 10-minute wash (Fig. 1C, right). The prolongation of τ_{slow} did not significantly affect the response area (control, 7591 ± 1642 pA* ms; SAS, 9858 ± 3124 pA* ms, p = 0.5).

To understand if SAS alters basal synaptic transmission, we compared the frequency and amplitude of sEPSCs and sIPSCs before and after application of SAS. Statistical analyses show significantly smaller sEPSC amplitudes (control: 18 ± 3 pA; SAS: 14 ± 2 pA, p = 0.02, Fig 1G) and a decrease in the frequency (control: 4.1 ± 0.7 Hz; SAS: 2.7 ± 0.5 Hz, p = 0.02, Fig 1H). For sIPSCs, we found a significant decrease in the frequency (control: 15 ± 2 pA; SAS: 9 ± 1.2 pA, p = 0.04, Fig 1G) but no change in the amplitude (control: 31 ± 9 pA; SAS: 24 ± 5 pA, p = 0.5, Fig 1H) in response to SAS.

3.3 Sulfasalazine decreases NMDAR-mediated currents

We wanted to test the effect of SAS on NMDA and AMPA receptor-mediated transmission during an evoked synaptic event. At a holding potential of -40 mV and in the presence of Bic and CNQX, to block $GABA_A$- and AMPA receptor-mediated currents respectively, the resulting NMDAR-mediated events were inward currents. Infusion of SAS resulted in a significant reduction in NMDA receptor-mediated currents (control: 97.93 ± 4.01 pA; SAS: 63.72 ± 21.01 pA, p < 0.001, Fig. 2A, B). We also tested the effect of another SXC inhibitor, S-4-CPG (100 μM), which resulted in a similar significant reduction in NMDA receptor-mediated current amplitude as SAS (control: 101.10 ± 2.82 pA; S-4-CPG: 61.74 ± 8.51 pA, p = 0.004, Fig. 2C, D). Co-application of S-4-CPG and SAS did not result in further decrease of NMDA receptor-mediated current (S-4-CPG: 61.74 ± 8.51 pA; S-4-CPG+SAS: 64.74 ± 10.53 pA, p = 0.69, Fig. 2C, D). To examine the effects of SAS on AMPA receptor-mediated currents, we recorded eEPSCs in the presence of Bic and APV (Fig. 2E, left), an NMDA receptor antagonist. We did not observe a significant change

in AMPA receptor-mediated eEPSCs (control: 101.16 ± 9.63 pA; SAS 89.98 ± 21.48 pA, p = 0.23, Fig. 2E, F). These results indicate that SAS attenuates eEPSCs primarily via a reduction in NMDA receptor-mediated currents, supporting previous *in vitro* studies describing the NMDA antagonistic properties of SAS[130,131].

3.4 Sulfasalazine decreases Mg^{2+}-free-induced cortical network hyperexcitability

The principle objective of this study was to determine whether inhibition of SXC, via SAS, can be explored as a novel therapeutic target for the treatment of acquired epilepsies. To this end, we used the SXC inhibitor SAS to question whether SAS could modulate epileptiform activity in distinct pharmacologically-induced hyperexcitability models. Bath application of SAS reduced the amplitude of Mg^{2+}-free-induced epileptiform discharges but unveiled lower amplitudes and shorter interictal events (Fig. 3A). Although the number of events did not significantly change with the addition of SAS (Mg^{2+}-free: 25.83 ± 16.58; SAS: 36.33 ± 26.34, p = 0.48, Fig 3B left), SAS significantly reduced the duration of the elicited events (Mg^{2+}-free: 4.13 ± 3.27 s; SAS: 0.55 ± 0.14 s, p = 0.04, Fig 3B right). Next, we assessed the effect of SAS on cortical network activity by using VSD recordings, which detects the spatiotemporal spread of neuronal network activity[132,133]. In the presence of the VSD RH-414, epileptiform network activity was elicited by intracortical stimulation in layer IV in cortical slices. Removal of Mg^{2+} from the recording solution causes an increase in the spread of VSD response. An example of Mg^{2+}-free-induced spatial dynamics of the VSD response is shown in Figure 3C (left). Each panel shows the spatial distribution and amplitude of dye signals at a given time point. Application of SAS for 30 minutes significantly decreased the peak amplitude (Fig. 3C, D, $p < 0.001$) and the spread of the VSD signals (Fig. 3C, D, $p < 0.001$) of Mg^{2+}-free-induced cortical network activity.

3.5 Sulfasalazine decreases bic-induced epileptiform activity and completely blocked 4-AP-induced network hyperexcitability

As SAS can act as a non-competitive NMDA receptor antagonist[131] and the Mg^{2+}-free solution induces epileptiform activity by removing the Mg^{2+} block from NMDA receptors, we wanted to evaluate the efficacy of SAS on other models of hyperexcitability. To test this, $GABA_A$ receptor-mediated inhibition was blocked by the addition of Bic to the perfusate, greatly enhancing the duration and lateral spread of the VSD signals, which is reflective of network hyperexcitability. In VSD recordings application of SAS significantly decreased the peak amplitude (Fig. 4A, B, $p < 0.001$) and spread (Fig. 4A, B, $p < 0.001$) of bic-induced network hyperactivity. On the other hand, in whole-cell recordings, SAS did not change the number of epileptiform discharges (Bic: 13.14 ± 7.67; SAS: 13.43 ± 7.52, $p = 0.85$, Fig 4C, D), but did significantly reduce the duration of the events (Bic: 2.21 ± 1.86 s; SAS 0.82 ± 1.00 s, $p = 0.01$, Fig 4C, D). Next, we tested the effects of SAS on epileptiform activity induced by application of 4-AP which blocks voltage-activated K^+ channels. In VSD recordings, 4-AP augmented the spatiotemporal spread of activity across the cortex. SAS significantly reduced the peak amplitude, indicated by the decrease in warmer colors (Fig. 5A, B, $p < 0.001$) and responses were restricted to the vicinity of the stimulation (Fig. 5A, B, $p < 0.001$). In whole-cell recordings, 4-AP-induced events which were completely blocked by SAS (4-AP: 93 ± 66.62; SAS: 0.5 ± 0.84, $p = 0.02$, Fig 5C, D) at the end of the recording. The duration of the few remaining events significantly decreased (4-AP: 2.16 ± 1.00 s; SAS: 0.14 ± 0.22 s, $p = 0.005$, Fig 5C, D) before being blocked at the end of the recording. Together these findings suggest that SAS can decrease the spread of epileptiform activity induced by different pharmacological agents, with distinct mechanism of action.

3.6 The effect of co-application of SAS and AEDs on cortical network activity

As polypharmacy is increasingly used in the management of intractable epilepsy, we examined whether co-application of a clinically approved AED and SAS would result in synergistic anti-epileptic effects compared to the AED alone. In VSD recordings, bath infusion of LEV to 4-AP-induced network activity (Fig. 6A, left and middle) resulted in a significant decrease in peak amplitude (Fig. 6A, B, $p < 0.001$) and spread (Fig. 6A, B, $p < 0.001$) of network activity, yet co-application of SAS with LEV (Fig. 6A, right) did not result in a significant change in amplitude peak (Fig. 6A, B, $p > 0.05$) or spread (Fig. 6A, B, $p > 0.05$) of network response. Similarly, when LEV was applied to Mg^{2+}-free-induced epileptiform activity (Fig. 6C, left and middle) it significantly decreased the peak amplitude (Fig. 6C, D, $p < 0.001$) and spread (Fig. 6C, D, $p < 0.001$) of network activity. However, co-application of SAS with LEV in Mg^{2+}-free (Fig. 6C, right) ACSF did not result in a significant change in peak amplitude (Fig. 6C, D, $p > 0.05$) and spread (Fig. 6C, D, $p > 0.05$) of neuronal network activity. We next examined the synergistic effects of SAS with another clinically approved AED, TPM. In the presence of 4-AP, application of TPM (Fig. 6E, left and middle) decreased the peak amplitude (Fig. 6E, F, $p < 0.001$) and spread (Fig. 6E, F, $p < 0.001$) of VSD response. Co-application of SAS with TPM (Fig. 6E, right) resulted in a vast additional reduction of peak amplitude (Fig. 6E, F, $p < 0.05$) and spread (Fig. 6E, F, $p < 0.05$) of 4-AP-induced VSD signal, compared to the effects of TPM alone. Altogether, our results indicate that SAS significantly reduces the spatiotemporal spread of cortical network activity in all three hyperexcitability models. In addition, concomitant use of TPM and SAS resulted in additional anti-epileptic effects compared to the use of TPM alone.

4 Discussion

Recent studies demonstrate that SAS is involved in modulating glutamate levels. We found that SAS modulates both evoked excitatory and inhibitory postsynaptic currents. We also show

that SAS can decrease network hyperexcitability in three pharmacologically-induced models. Furthermore, SAS is more efficacious in inhibiting 4-AP-induced network activity compared to the currently prescribed AED TPM.

We first used patch-clamp recordings to explore the effect of SAS on evoked EPSCs in layer II/III pyramidal neurons and observed that SAS (as well as S-4CPG) decreased EPSC amplitude via a reduction in NMDAR-mediated currents. These results support previous *in vitro* studies which sought to characterize the NMDA antagonistic properties of SAS[130,131]. Our results show that SAS decreased both the amplitude and frequency of sEPSCs, which suggests that it could be acting via both pre – and postsynaptic mechanisms. Surprisingly we found that while SAS decreased the amplitude of eIPSCs, it significantly prolonged the τ_{slow}. The increase in the τ_{slow} could have a significant inhibitory effect, by prolonging inhibitory currents, but also questions the possible effect of SAS on GABA uptake mechanisms. More studies are needed to better understand the effects of SAS on inhibition.

The objective of this study is to elucidate the global effects of SAS-mediated inhibition of SXC in distinct models of hyperexcitability, as a proxy for the hyperexcitable brain microenvironment in patients with epilepsy. We used acute cortical slices from C7Bl6 mice bathed in Mg^{2+}-free, bic or 4-AP containing ACSF to simulate cortical network hyperexcitability. Under these conditions we found that SAS significantly reduced the amplitude and spread of evoked epileptiform activity in all hyperexcitability models tested. Notably, we observed that in VSD recordings SAS reduced the optical response in both Mg^{2+}-free and bic-containing ACSF, but SAS did not reduce the number of epileptiform events in whole-cell patch clamp recordings. Instead, SAS decreased the duration of the epileptiform events in all the models tested. The latter is similar to the effect of AEDs on 4-AP-induced epileptiform activity, where ictal events were abolished

but not interictal events[134,135]. As reported by D'Antuono et al. (2010), epileptiform discharges induced by 4-AP in the entorhinal cortex were sensitive to carbamazepine and TPM, by blocking ictal events but not interictal. However, in our study, SAS surprisingly completely blocked all 4-AP-induced epileptiform activity in the prefrontal cortex. This was observed at the single cell level where application of SAS first caused a decrease in the duration of epileptiform events and later completely blocked epileptiform events and also at the network level by significantly decreasing VSD optical signals. In the presence of bic-induced epileptiform events, SAS decreased the spread of the VSD optical signal but not the number of epileptiform events in whole cell recordings. During these experiments we observed either an increase or no change in the number of events, but there was a consistent decrease in the duration of the events in all experiments. When hyperexcitability was induced by Mg^{2+}-free solution, the spread and duration of VSD optical signal was decreased. Under the same conditions, in whole-cell recordings SAS significantly decreased the duration of epileptiform events and increased the number of events, supporting previous findings of blocking ictal but not interictal events[5]. Differential changes in the parameters of epileptiform activity have been described in the entorhinal cortex of kainate-treated rats in response to several AEDs[136]. The findings from these experiments validate SAS's ability to decrease hyperexcitability induced by different mechanisms.

Based on SAS's significant effect on 4-AP-induced epileptiform events we questioned how it compares to currently prescribed AEDs. We found that LEV significantly decreased the spread and duration of both 4-AP and Mg^{2+}-free-induced VSD optical signal and co-application of SAS did not significantly affect the small remaining VSD optical signal. However, we found that while TPM partially decreased the spread and duration of VSD optical signal induced by 4-AP, it was to a lesser degree compared to the inhibition by LEV. When SAS was later co-applied with TPM, it

caused a significant decrease in the remaining VSD optical signal. It is worth noting that in the present study a single drug concentration of SAS and AEDs was chosen based on previous studies and a more rigorous pharmacological study would be necessary to fully compare the efficacy of SAS to AEDs.

Although it is estimated that 1-in-26 people develop epilepsy within their lifetime[137], current AEDs are not effective for a third of affected patients[14]. This unmet need has led to the development of seventeen clinically approved AEDs in the last 30 years[138]. The rise in the number of clinically available AEDs resulted in the use of polytherapy to address drug-resistant epilepsies. However, the efficacy of polytherapy has been debated as different studies have demonstrated mixed results[139-141]. One possible explanation for the limited efficacy of polytherapy in drug-resistant epilepsies may be due to current AEDs targeting primarily neuronal processes. As more evidence regarding the contributions of glial processes in epileptogenesis continues to become unveiled[142-145] the prospect of novel, non-neuronal targets involved in seizure generation and epileptogenesis is encouraging. Knowing that increased SXC expression has been found in human epileptic tissue[24], and the strong link between aberrant SXC expression in tumor-associated epilepsy, further studies on SXC as a target for acquired epilepsy are warranted. SXC's inhibition by SAS provides a novel, non-neuronal treatment modality for decreasing release of excitatory glutamate in the brain.

Based on our findings, we propose that SAS inhibits SXC primarily on astrocytes to cause a decrease in ambient, extracellular glutamate concentrations, that results in decreased activity of extrasynaptic NMDARs leading to suppression of slow-transient currents. Pharmacological inhibition of SXC in rats reduces extracellular glutamate by 60%[146] and genetic knock-out of SXC

in mice and drosophila results in a significant decrease in extracellular glutamate[54,147]. More studies are required to determine specific changes on glutathione.

In conclusion, we demonstrate that SAS can decrease three pharmacologically-induced models of cortical network hyperexcitability. Finally, SAS was more efficacious in decreasing the spread and duration of 4-AP-induced VSD optical response compared to the currently prescribed AED TPM, suggesting that it could be explored as a potential adjuvant treatment for seizures.

Acknowledgments

This work was supported by US National Institutes of Health grants RO1-NS052634, 5RO1-NS036692, and R01CA227149 and start-up funds from the College of Agricultural and Life Sciences and the College of Science at Virginia Tech, United States. We thank Dr. John J. Hablitz at the University of Alabama at Birmingham for the use of his voltage-sensitive dye setup.

Disclosures

The authors have no conflict of interest to report. We confirm that we have read the Journal's position on issues involved in ethical publication and affirm that this report is consistent with those guidelines.

Figures

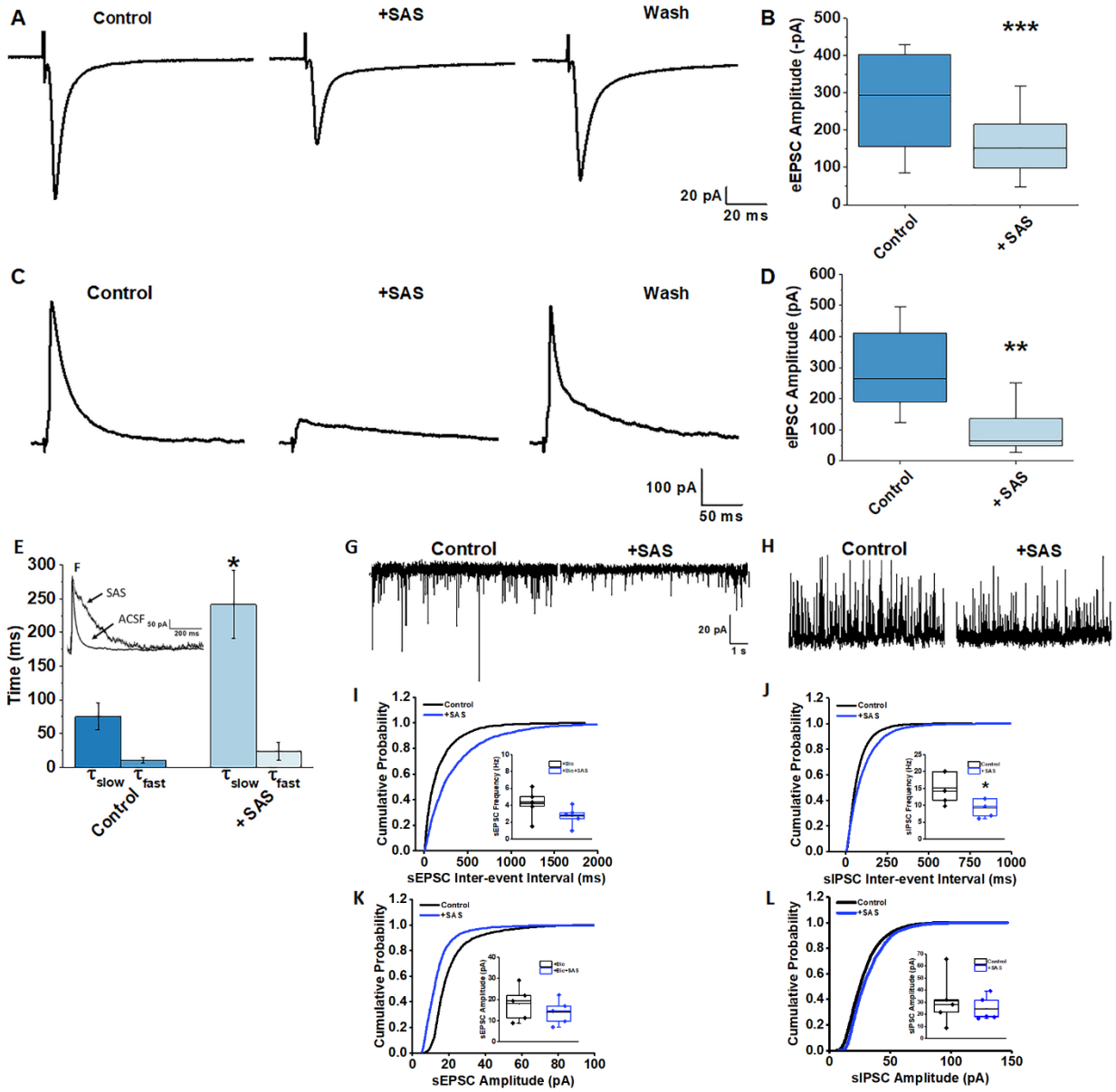

Figure 1: SAS decreases synaptic responses in layer II/III pyramidal cells. (A) Representative traces of eEPSCs of a layer II/III pyramidal cell in an acute cortical slice before (left), during a 10-minute application of SAS (middle) and after a wash (right). (B) Quantitative summary of the eEPSC amplitude before and in the presence of SAS. *** = significantly different than control, n = 9, p = 0.001. (C) Representative traces eIPSCs of layer II/III

pyramidal cells in an acute cortical slice before (left), during a 10-minute application of SAS (middle) and after a wash (right). (D) Quantitative summary of the eIPSC amplitude. ** = significantly different than control, n = 6, p = 0.003. (E) Quantitative summary of τslow and τfast eIPSC decay kinetics before and in the presence of SAS. * = τslow + SAS is significantly different than τslow Control, n = 6, p = 0.03. (F, inset) Normalized eIPSC traces from control (ACSF) and SAS treated slices. Representative traces of sEPSCs (G) and (spontaneous inhibitory postsynaptic currents) sIPSCs (H) of layer II/III pyramidal cells in an acute slice before (left) and during SAS application (right). (I) Cumulative probability plot and average values (inset) of sEPSC frequency and amplitude (J). (K) Cumulative probability plot and average values (inset) of sIPSC frequency and amplitude (L).

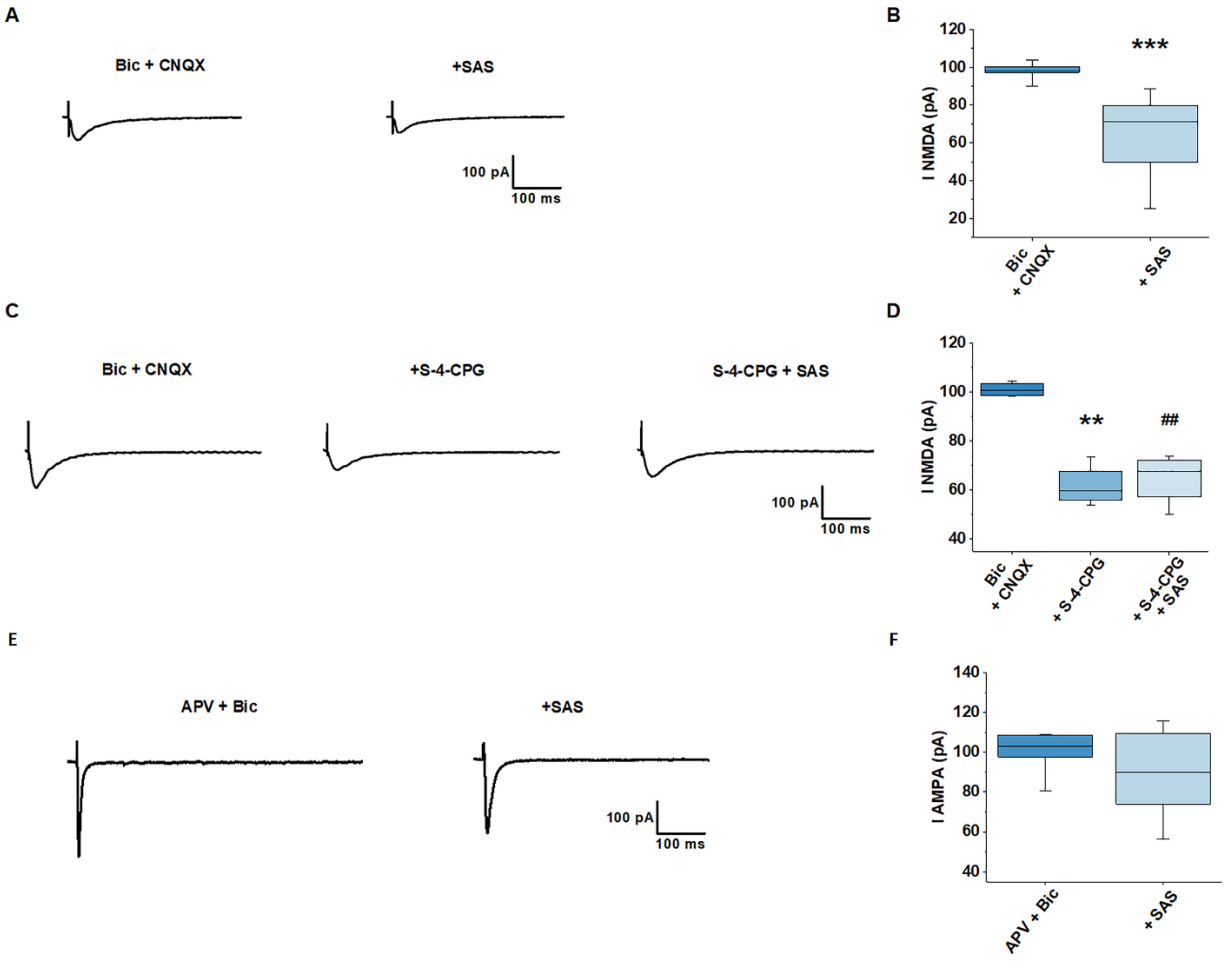

Figure 2: SAS decreases NMDAR-mediated currents. (A) Representative traces of isolated NMDAR-mediated currents before (left) and after application of SAS (right). (B) Quantitative summary of isolated NMDA EPSCs before and after SAS application. *** = SAS application significantly different than bic + CNQX, n = 13, $p < 0.001$ (C) Representative traces of isolated NMDAR-mediated currents (left), in the presence of S-4-CPG (middle) and during co-application of SAS (right). (D) Quantitative summary of isolated NMDA EPSCs under control conditions, in the presence of S-4-CPG and with co-application of S-4-CPG + SAS. ** = S-4-CPG application significantly different than bic + CNQX, n = 4, $p = 0.004$. # = S-4-CPG + SAS co-application significantly different than bic + CNQX, n = 4, $p = 0.01$ (E) Representative traces

of isolated AMPAR EPSCs (left) and response to SAS application (right). (F) Time course experiment showing the effect of SAS on AMPA EPSCs amplitude. No significant change was detected (n = 8, p = 0.23).

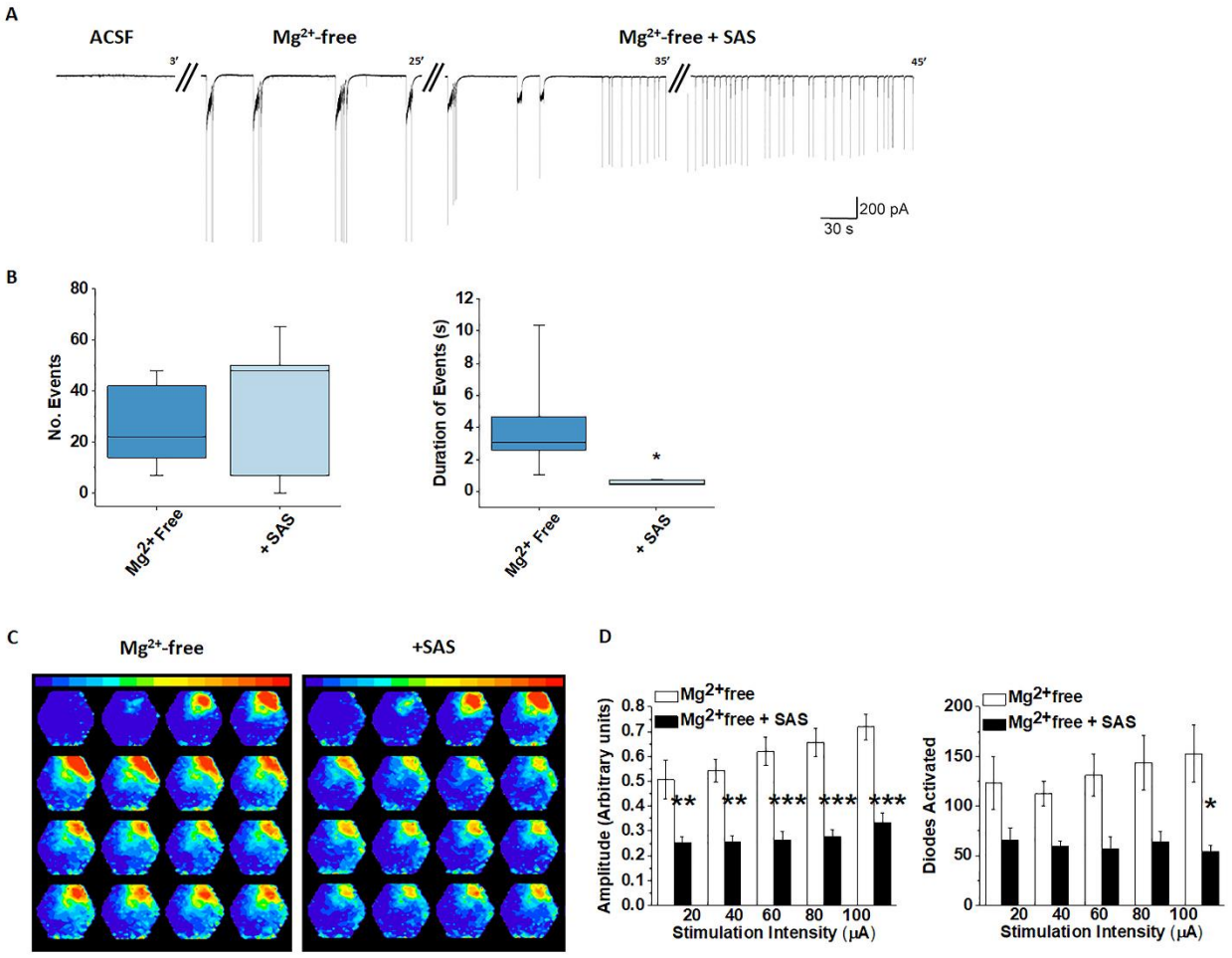

Figure 3: Effects of SAS on Mg2+-free-induced epileptiform activity and VSD imaging network response. (A) Representative traces of whole-cell patch clamp recordings depicting a decrease in Mg2+-free-induced ictal events with SAS, but not interictal events. (B) Quantitative summary of the number (left) (n = 6, p = 0.48) and duration (right) of epileptiform events detected in whole-cell patch clamp recordings. * = SAS application significantly different than Mg2+-free, n = 6, p = 0.04. (C) Representative optical recordings depicting the spatiotemporal

spread of activity evoked in cortical slices in Mg2+ free perfusate (left) and 30 min after the application of SAS (right). The pseudocolor images and dye signals depict a decrease in the large spread in VSD signal in the presence of SAS. (D) Quantitative summary of the amplitude (left) and spread (right) of Mg2+-free-induced VSD signals. SAS application significantly decreased the response amplitude and number of diodes activated between Mg2+-free and Mg2+-free + SAS, $n = 6$, $p < 0.001$. Additionally, significant condition-by-stimulation intensity interactions between Mg2+-free and Mg2+-free + SAS means were also found. * = $p = 0.01$ ** = $p < 0.01$, *** = $p < 0.001$.

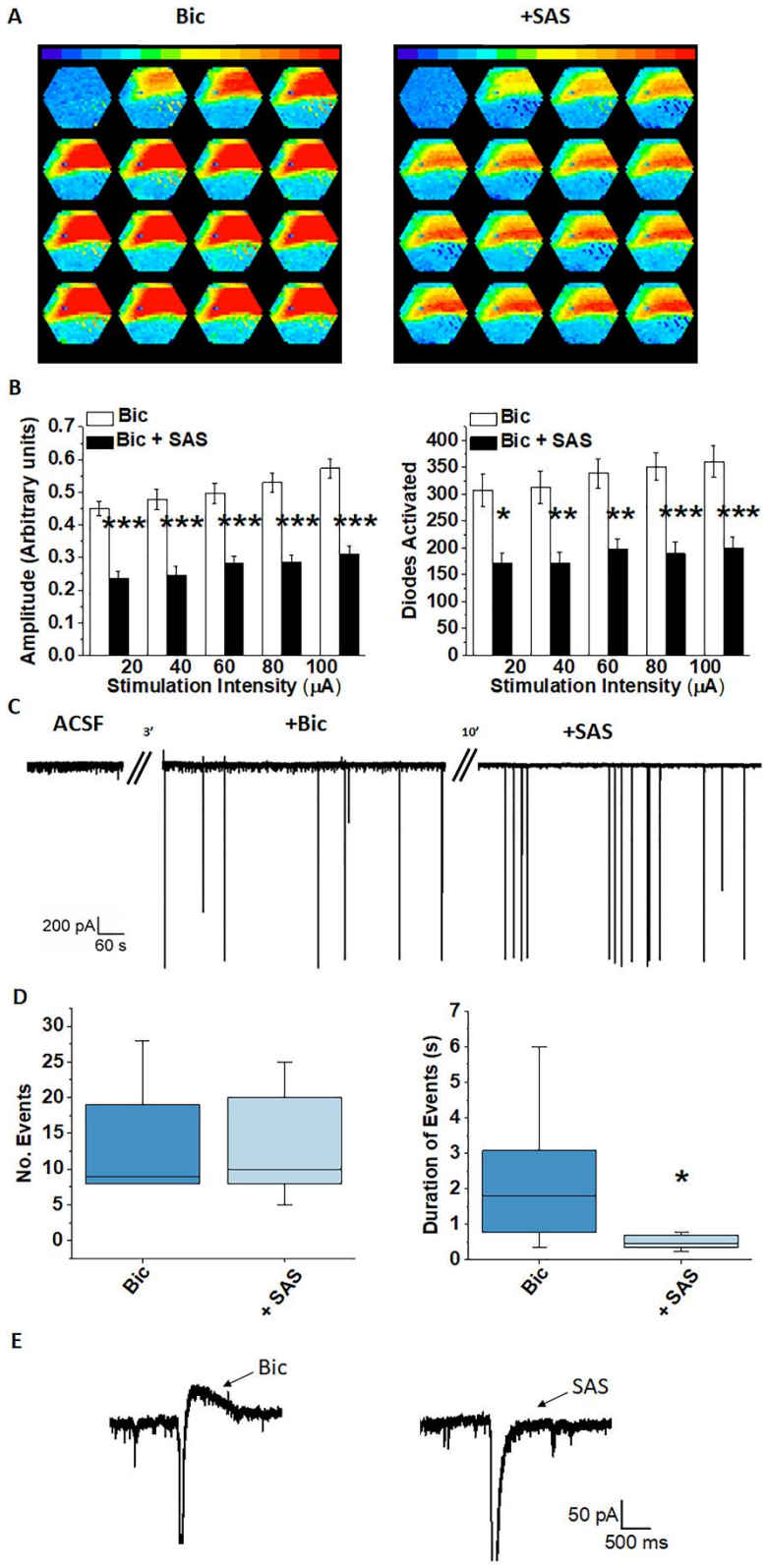
A
Bic
+SAS
B
Bic
Bic + SAS
Amplitude (Arbitrary units)
Stimulation Intensity (μA)
Diodes Activated
C
ACSF
+Bic
+SAS
200 pA
60 s
D
No. Events
Duration of Events (s)
Bic
+SAS
E
Bic
SAS
50 pA
500 ms

Figure 4: SAS decreases spatiotemporal spread of bic-induced network activity and epileptiform events. (A) A pseudocolor map of the spatiotemporal patterns of activity evoked by intracortical stimulation in the presence of bic (left) and after application of SAS (right) at the same stimulation intensity. (B) Quantitative summary of the amplitude and spread of bic-induced epileptiform activity using VSD recordings. Application of SAS significantly decreased the response amplitude and number of diodes activated between Bic and Bic + SAS, $n = 6$, $p < 0.001$. Significantly different condition-by-stimulation intensity interactions between Bic and Bic + SAS means were also found. * = $p = 0.01$ ** = $p < 0.01$, *** = $p < 0.001$. (C) Representative traces of whole-cell patch clamp recordings in ACSF (left), Bic (middle) and SAS (right). (D) Quantitative summary of the number and duration of epileptiform events detected in whole-cell patch clamp recordings. * = significantly different than Bic, $n = 7$, $p = 0.01$. E) Magnified bic (left) and SAS (right) traces during an epileptiform event.

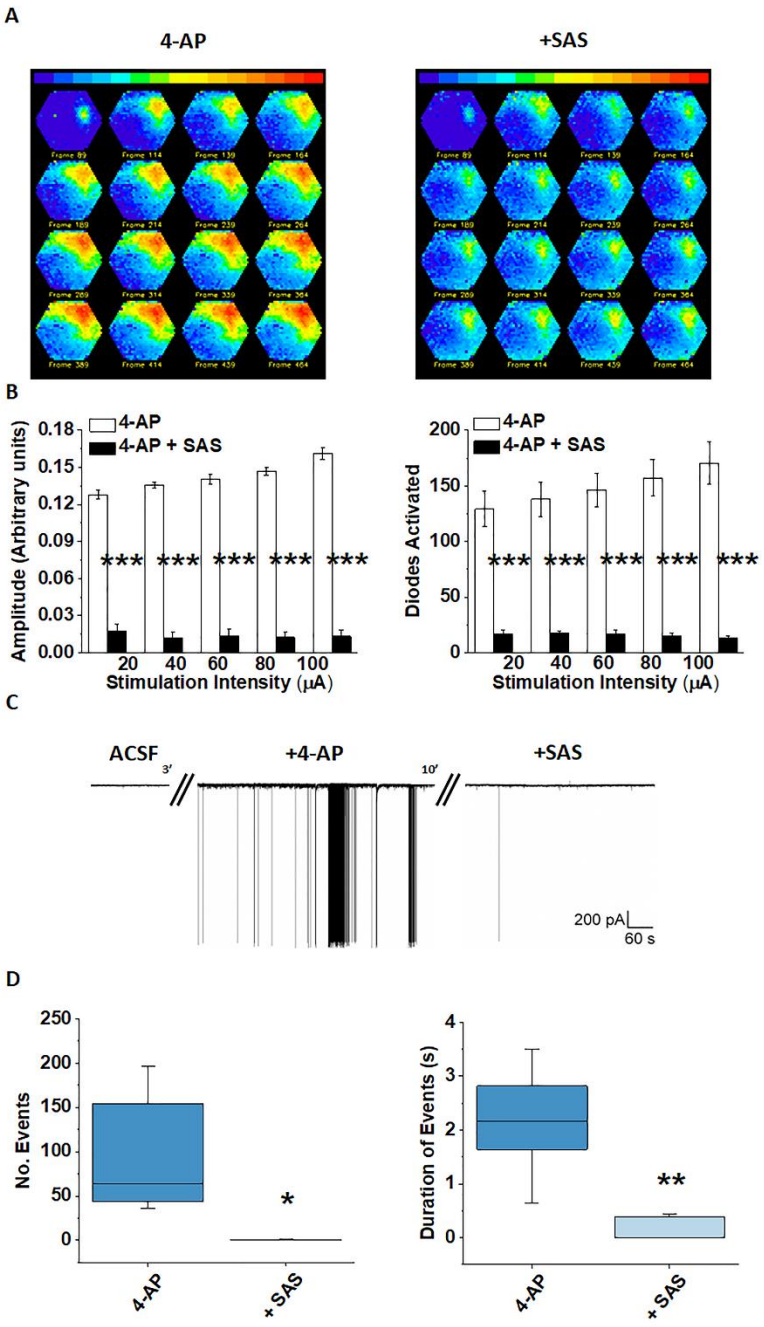

Figure 5: SAS blocks 4-AP-mediated epileptiform and VSD network response. (A) Representative spatiotemporal patterns of activity evoked by a single pulse stimulation in the presence of 4-AP (left) and after application of SAS (right). SAS exhibits a net inhibitory effect on the activity evoked by 4-AP. (B) Summary of the amplitude and spread of 4-AP-mediated

epileptiform activity using VSD recordings. Application of SAS significantly decreased the response amplitude and number of diodes activated between 4-AP and 4-AP + SAS, $n = 8$, $p < 0.001$. Significant condition-by-stimulation intensity interactions between 4-AP and 4-AP + SAS means were also found. *** = $p < 0.001$. (C) Specimen recording showing a complete block of ictal and interictal 4-AP-induced epileptiform activity (middle) upon application with SAS (right). (D) Quantitative summary of the number and duration of epileptiform events detected in whole-cell patch clamp recordings. * = SAS application significantly different than 4-AP, $p = 0.02$ ** = SAS significantly different than 4-AP, $p = 0.005$. $n = 6$.

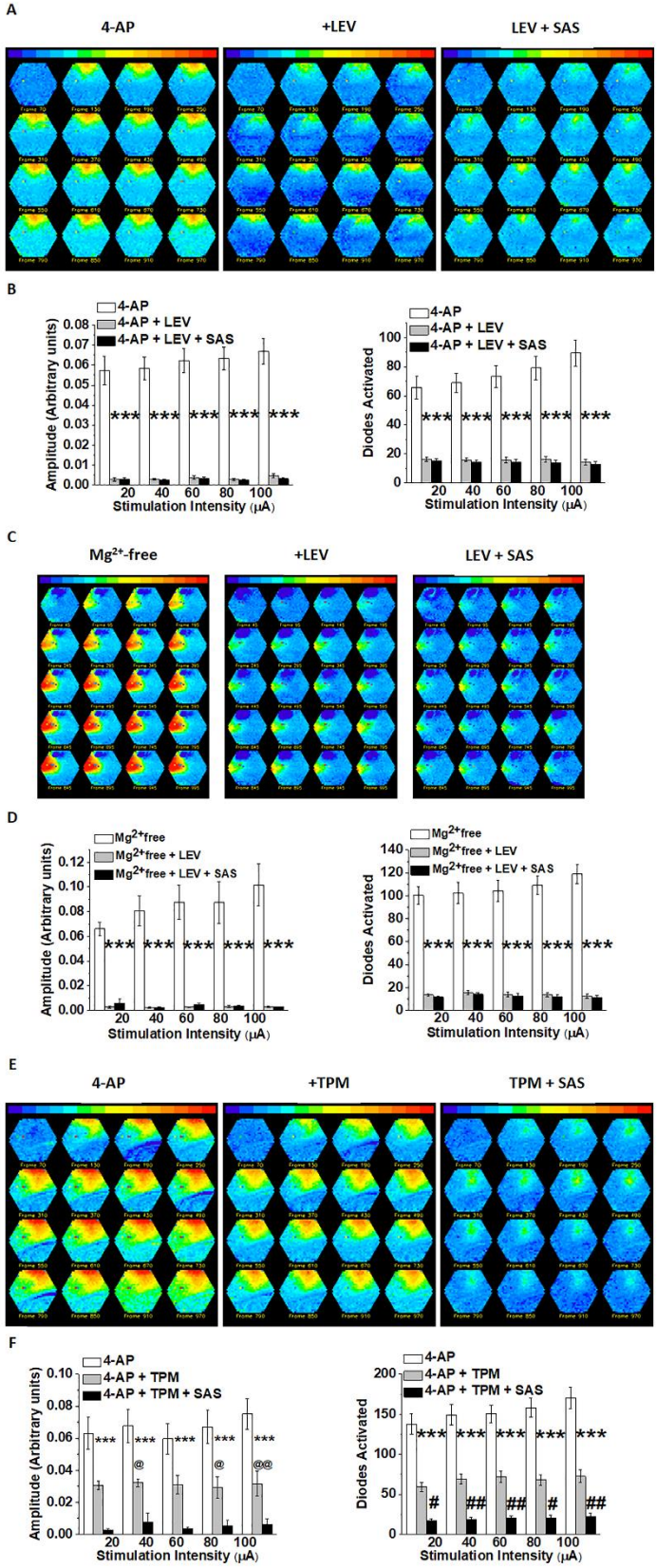
A
4-AP
+LEV
LEV + SAS
B
4-AP
4-AP + LEV
4-AP + LEV + SAS
Amplitude (Arbitrary units)
Diodes Activated
Stimulation Intensity (μA)
C
Mg2+-free
+LEV
LEV + SAS
D
Mg2+free
Mg2+free + LEV
Mg2+free + LEV + SAS
Amplitude (Arbitrary units)
Diodes Activated
Stimulation Intensity (μA)
E
4-AP
+TPM
TPM + SAS
F
4-AP
4-AP + TPM
4-AP + TPM + SAS
Amplitude (Arbitrary units)
Diodes Activated
Stimulation Intensity (μA)

Figure 6. Comparison of VSD signals in response to co-application of AEDs and SAS. (A) Spatiotemporal patterns of activity evoked in the upper cortical layers in 4-AP (left), after application of LEV (middle) and after co-application with SAS (right). (B) Quantitative summary of the amplitude and spread of 4-AP-mediated VSD signal in the presence of LEV and LEV + SAS (n = 9). A significant decrease was found in the response amplitude and number of diodes activated between the different conditions (4-AP, 4-AP + LEV, 4-AP + LEV + SAS). $P < 0.001$. Significant condition-by-stimulation intensity interactions in the means of the response amplitude and number of diodes activated between 4-AP and 4-AP + LEV, and, 4-AP and 4-AP + LEV + SAS, were also found. *** = $p < 0.001$. No significant difference was found between LEV and co-application of LEV + SAS (C) Network activity evoked in cortical layer II/III in Mg2+-free ACSF (left), after application of LEV (middle) and following co-application of SAS (right). (D) Summary bar graphs of the amplitude and spread of Mg2+-free epileptiform activity in the presence of LEV and LEV + SAS (n = 9). A significant decrease in the response amplitude and number of diodes activated between the different conditions (Mg2+-free, Mg2+-free + LEV, Mg2+-free + LEV + SAS). $P < 0.001$. Significant condition-by-stimulation intensity interactions in the means of the response amplitude and number of diodes activated between Mg2+-free and Mg2+-free + LEV, and, Mg2+-free and Mg2+-free + LEV + SAS, were also found. *** = $p < 0.001$. No significant difference was found between LEV and co-application of LEV + SAS (E) Spatiotemporal patterns of activity evoked in 4-AP (left), after application of TPM (middle) and after co-application of SAS (right). (F) Summary bar graphs of the amplitude and spread of 4-AP mediated epileptiform activity in the presence of TPM and TPM + SAS (n = 7). Significant decreases were found in the response amplitude and number of diodes activated between the different conditions (4-AP, 4-AP + TPM, 4-AP + TPM + SAS). $P < 0.001$. Significant condition-

by-stimulation intensity interactions in the means of response amplitudes at stimulation intensities of 20, 80 and 100µAs between 4-AP and 4-AP + TPM, were also found. @ = $p < 0.05$, @@ = $p = 0.002$. Interactions in amplitude response between 4-AP and 4-AP + TPM + SAS were significant at all stimulation intensities, *** = $p < 0.001$. No significant interaction was found between 4-AP + TPM and 4-AP + TPM + SAS response amplitudes. Significant condition-by-stimulation intensity interactions were found in the number of diodes activated between 4-AP and 4-AP + TPM, and, 4-AP and 4-AP + LEV + SAS, *** = $p < 0.001$. Additionally, significant interactions between the number of diodes activated in 4-AP + TPM and 4-AP + TPM + SAS were found at all stimulation intensities. # = $p < 0.05$, ## = $p < 0.01$.

Chapter 4

This chapter is formatted as a manuscript in preparation for journal submission

Sulfasalazine decreases astrogliosis-mediated seizure burden

Introduction

All epilepsies are characterized by the occurrence of spontaneous, recurrent seizures, however, the wide spectrum of underlying etiologies and severity of disease among people living with epilepsy continues to challenge the development of broadly effective anti-epileptic drugs (AEDs)[9]. The past few decades have produced third-generation AEDs that have provided physicians more efficacious options for initial and adjunct therapies[148]. Most of these AEDs function through direct interactions with neuronal targets that work to either decrease excitatory or increase inhibitory neuronal mechanisms[149]. Despite continued development of novel AEDs, current treatment options fail 1-in-3 patients[2,28]. A statistic that has not significantly changed in over 50 years since a 1971 report on the clinical efficacy of AEDs stating the efficacy at the time to be lower than 70 – 80% [15,28].

These reports suggest that the pursuit of disease modifying therapies and AEDs that can provide relief to patients who currently have none may require the use of new epilepsy models and expanding the search for new drug targets beyond the neuron. One such target is system xc- (SXC), a covalently coupled protein complex made up of the 4F2 heavy chain (encoded by *SLC3A2)* and the cystine/glutamate exchanger (xCT) (encoded by *SLC7A11).* Although evidence of xCT expression has been found in cells throughout the body, investigations using xCT knockout mice ($xCT^{-/-}$) to validate expression patterns found that xCT protein expression in the CNS is limited to astrocytes and absent in neurons, oligodendrocytes and microglia[23]. Importantly, SXC activity has been shown to be a major determinant in setting the ambient, extracellular glutamatergic tone within the CNS. Two separate studies using (S)-4-carboxyphenylglycine (S-4-CPG) or antisense xCT to inhibit SXC found that SXC inhibition resulted in a 40-60% decrease in extracellular glutamate within the nucleus accumbens[3,4].

In addition to the role of SXC in determining ambient CNS glutamatergic tone in health, unregulated SXC activity has been linked to the generation of tumor-associated epilepsy in glioblastomas. Studies from our lab have revealed that aggressive glioblastomas overexpress SXC and have elevated peritumoral extracellular glutamate levels leading to neuronal excitotoxicity, development of tumor-associated epilepsy and poor patient survival[5-7]. Intriguingly, SXC inhibition using sulfasalazine (SAS), an FDA approved drug used to treat inflammatory bowel disease, was found to decrease epileptiform activity both in *in vitro* and *in vivo* glioblastoma models. Recently, we have also demonstrated that SAS is capable of significantly decreasing the frequency and/or amplitude of evoked excitatory post synaptic currents in multiple *in vitro* models of hyperexcitability[55]. Taken together, investigations of SXC inhibition to lower extracellular glutamate concentrations and decrease neuronal hyperexcitability in the setting of epilepsy appears to be a suitable strategy. However, in contrast to tumor-associated epilepsy, other forms of acquired epilepsy do not have a large concentration of mutated cells that overexpress SXC and consequently elevate extracellular ambient glutamate concentrations. How efficacious would SXC-directed therapy be in other forms of epilepsy?

To help answer this question our study uses the β1-integrin knockout (B1KO) mouse model of astrogliosis mediated epilepsy. Previously, our lab characterized the effects of knocking out radial glial cell β1-integrin, a cell adhesion molecule, in mice[26,27]. The B1KO model uses a cre-lox system to conditionally delete β1-integrin in astrocytes by coupling cre with GFAP expression. Interestingly, at 2 weeks of age B1KOs and controls appear phenotypically normal, however, by 4 weeks of age B1KOs develop widespread, chronic astrogliosis in the brain which persists beyond 6 months of age. Importantly, loss of astrocytic β-1 integrin did not result in gross structural abnormalities, marked inflammation or decreases in the number of neurons. In

response to chronic astrogliosis, B1KOs were shown to develop spontaneous seizures by 6 weeks of age.

Common animal models of epilepsy that have aided the development of current AEDs use chemoconvulsants, such as kainic acid or pilocarpine, or electrical stimulation to induce status epilepticus which ultimately reproduces features commonly seen in human temporal lobe epilepsy [150]. Induction of status epilepticus, a life-threatening condition, results in significant neuronal excitotoxicity, inflammation and hippocampal sclerosis which can complicate investigations of epileptogenesis and novel therapeutics by introducing a host of confounding factors such as blood brain barrier disruption, immune infiltration and release of inflammatory cytokines[150]. Although the B1KO model is not known to emulate any known human disease, this unique model provides a platform to study the isolated relationship between astrogliosis and the development of epilepsy.

In this study, we used 24/7 video-electroencephalogram (video-EEG) and electrophysiology to further characterize the B1KO model and to test the efficacy of SAS in reducing astrogliosis mediated seizure burden. We found that 100% of B1KOs exhibited spontaneous recurrent seizures, in contrast to the previously published incidence of 58%[27] in which continuous 24/7 video-EEG was not utilized. Additionally, one week of twice daily SAS administration was found to significantly reduce the seizure burden of B1KOs and acutely decrease EEG activity when administered. Lastly, we used acute slice electrophysiology to examine the behavior and properties of cortical pyramidal neurons in B1KOs and a B1KO - $xCT^{-/-}$ double knockout cross. These experiments revealed that mice lacking functional SXC exhibited neuronal hyperpolarization compared to controls.

Materials and Methods

Animals

Animals were housed and handled according to the guidelines of the National Institutes of Health Committee on Laboratory Animal Resources. Prior approval of the Virginia Tech Institutional Animal Care and Use Committee was obtained for all experimental protocols. All efforts were made to minimize pain. Experiments were performed using 5 to 13-week-old male and female B1KO (FVB/N background), $xCT^{-/-}$ (C57BL/6 background) and B1KO- $xCT^{-/-}$ cross mice.

EEG electrode surgical procedure

All animal procedures were approved by the Virginia Tech Institutional Animal Care and Use Committee and Institutional Biosafety Committee and were carried out in accordance with the National Institutes of Health Guide for the Care and Use of Laboratory Animals. 5 – 7-week-old B1KOs were set up on a stereotaxic apparatus (David Kopf Instruments) and anesthetized using 1.5 – 3.5% isoflurane via nose cone throughout the procedure. First, the scalp over the surgical site was depilated using topical hair-removal cream (Nair) and sterilized with ethanol and betadine. Next, a ½-1-centimeter single incision is made in the scalp, front to back, using a scalpel. Cranial sutures then are located, and 6 burr holes are drilled through the skull without puncturing the brain using a 1 mm drill tip. Three small stainless-steel screws are placed into three outer burr holes. Then, 2 EEG lead wires and 1 ground wire, all cut to 2 mm, are inserted into the remaining three burr holes and dental acrylic is applied to form a stable cap on the skull that cements the electrodes in place. The EEG lead wire holes are placed 2.5mm caudal to the bregma, 2.0mm laterally and 1.5mm dorsoventral using a stereotax. The EEG ground wire hole is placed 1.0 mm caudal to bregma, 1.0mm laterally and in contact with the dura mater over the surface of the cortex. When

the acrylic has dried, the skull is swabbed with povidone-iodine and the scalp is closed with surgical adhesive.

Video-Electroencephalography (video-EEG)

After 5-7 days of recovery from the surgical electrode implantation procedure, mice were monitored 24/7 via video-EEG for a total of 2-3weeks per mouse. EEG recordings were obtained and analyzed using the MP160 data acquisition system and AcqKnowledge 5.0 software from BIOPAC Systems, Inc. Video recordings were obtained using M1064-L network cameras (Axis Communications) and stored on an Amcrest DVR. Mice were connected to EEG100C amplifiers (BIOPAC) using custom-made six-channel cable connectors (363-000 and 363-441/6, Plastics 1) and six-channel rotating commutators (SL6C/SB, Plastics 1). All cables and electrical components were shielded to minimize electrical noise. Food and water were freely accessible to mice throughout the video-EEG recordings. EEG signals were bandpass filtered (high pass filter: 0.5Hz, low pass filter: 100Hz), amplified and digitized at a sampling frequency of 500Hz.

Seizure Analysis

Only behavioral, convulsive seizures were included in our analysis. Behavioral seizures were manually located on EEG recordings by an investigator blinded to genotype and treatment groups and subsequently confirmed using temporally aligned video recordings. Common electrographic seizure characteristics were used to identify potential seizures such as: pre-ictal low amplitude spikes that gradually increase in amplitude until ictal fast rhythmic spikes with amplitudes at least two times higher than baseline and lasting at least 5 seconds developed. Post-ictal suppression of EEG also occurs after convulsive seizures which correspond to behavioral arrest in mice. Seizure event duration was obtained using EEG and defined as the period of time from the start of ictal

fast rhythmic spiking until the end of the post-ictal suppression. Behavioral seizure severity was scored using a modified Racine scale with the following score definitions: 3 – rearing + forelimb clonus; 4 – rearing/falling + front-limb clonus; 5 – intense running/jumping with repeated falling and severe clonus. Due to the length of continuous recordings and free mouse movement some electrode caps became dislodged before the completion of the experiment. EEG recordings from mice with dislodged electrode caps were not used or analyzed. Only video-EEG recordings from mice that completed the entire experiment were analyzed.

SAS and saline treatment

SAS (Sigma) was solubilized in 0.1M NaOH and neutralized to pH 7.4 using 0.1M HCl for *in vivo* intraperitoneal injections at a dose of 400mg/kg. This dose was used due to its equivalence of doses taken by Crohn's disease patients. For sham injections, 0.9% sterile saline was used using an equivalent volume as the SAS group. During the treatment period mice were injected twice daily for 6 days and once in the morning of the 7^{th} day. Daily intraperitoneal injections were administered 8 hours apart between 8-10am and 4-6pm. Special care was given by investigators with extensive mouse handling experience to ensure the safety and health of mice after repeated intraperitoneal injections. Mice that developed significant bruising from repeated injections were removed from the experiment and analysis.

Acute slice preparation

Mice were anesthetized and decapitated and their brains were quickly removed and immersed in ice-cold cutting solution containing (in mM): 135 N-methyl-D-glucamine (NMDG), 1.5 KCl, 1.5 KH2PO4, 23 mM choline bicarbonate, 25 D-glucose, 0.5 mM CaCl2, 3.5 MgSO4 (Sigma-Aldrich). Coronal brain slices (300 μm) were made and recovered for 40-60 min in oxygenated recording

solution in mM: 125 NaCl, 3 KCl, 1.25 NaH_2PO_4, 25 $NaHCO_3$, 2 $CaCl_2$, 1.3 $MgSO_4$, 25 D-glucose at 32 °C and maintained at room temperature before recordings.

Whole-cell recordings

Individual brain slices were transferred to a recording chamber and continuously perfused (4ml/min) with oxygenated recording solution. Whole-cell recordings were conducted using borosilicate glass capillaries (KG-33 glass, Garner Glass) and filled with internal solution containing (in mM): 134 K-gluconate, 1 KCl, 10 HEPES, 2 mg-ATP; 0.2 Na-GTP and 0.5 ethylene glycol tetraacetic acid (EGTA). The pH was set to 7.24 with KOH, and the osmolality was measured (~290 mOsm/kg). All recordings were performed at 32 ± 1°C. Individual cells were visualized using a Zeiss Axioscope (Carl Zeiss, Thornwood, NY) microscope equipped with Nomarski optics with a 40X water immersion objective lens. Tight seals were made using electrodes with a 3–5-MΩ open-tip resistance. Signals were acquired from layer II/III pyramidal cells with an Axopatch 1B amplifier (Molecular Devices), controlled by Clampex 10 software via a Digidata 1440 interface (Molecular Devices).

Statistics

Two-sample Student's t test were used for means comparisons among the weekly seizure frequencies, percentage of seizure free days, seizure duration, seizure score, change in EEG power, resting membrane potentials and threshold current. Paired Student's t test was used for seizure frequency comparisons among paired saline and SAS treated B1KOs. Two-way ANOVA and Fisher's post-hoc test was used for means comparisons and interactions to determine action potential frequency significance in Figure 6. Statistics were generated and graphed using Origin 7.5 Pro software (Origin), significance set at $P < 0.05$. Figures display box-and-whisker plots

(minimum to maximum, median line) or histograms (mean ± standard error of mean). Values in the text report mean ± standard deviation.

Results

All B1KOs developed spontaneous recurrent seizures between 7 – 12 weeks of age

The original paper characterizing the development of spontaneous seizures in B1KOs reported seizure frequencies ranging from 0 – 0.249 seizures/hour[27] in mice between 4 weeks and over 6 months of age. One limitation of this previous study was the use of discontinuous video-EEG recordings resulting in total recording times ranging from 22 – 257.93 hours per mouse. To obtain a closer approximation of the baseline seizure burden in B1KOs we employed 24/7 video-EEG recordings in 2 or 3-week increments from B1KOs between 7 and 12 weeks of age. Using continuous video-EEG recordings we found that 100% of B1KOs (20/20) developed behavioral spontaneous recurrent seizures at a weekly seizure frequency between 0.029 – 0.040 seizures/hour (Figure 1). Using a heatmap to visualize the distribution of seizures over time (Figure 2) in this model it is apparent that B1KOs have "seizure clusters" or "acute repetitive seizures" which is a phenomenon commonly found in human epilepsy and associated with medically refractory epilepsy[151,152].

Sulfasalazine treatment decreases seizure burden in B1KOs

Previously we reported the ability of SAS to decrease cortical hyperexcitability in acute brain slices exposed to 3 distinct chemical hyperexcitability models[55]. Using the insights from this study, we set out to test whether SAS administration could decrease seizure burden *in vivo* using B1KOs. To this end, we used 24/7 video-EEG monitoring to continuously record B1KOs

and controls for 2-weeks, to establish a baseline seizure frequency per mouse, followed by 1-week of twice daily SAS (or saline sham) intraperitoneal injections (Figure 2).

Grouping the seizure frequency data into weeks (baseline = weeks 1 and 2; treatment = week 3), there was a significant increase in seizure burden between week 1 and week 3 of the B1KOs who received saline injections during the treatment week (week 1-baseline: 0.031 ± 0.016; week 3-saline: 0.049 ± 0.011 seizures/hour, $P = 0.019$). B1KOs treated with SAS throughout week 3 (week 3-SAS: 0.031 ± 0.023) retained a seizure burden similar to week 1 (Figure 3a). Additionally, there was a significant increase in the percentage of seizure-free days in the SAS group compared to both the baseline week 2 (week-3 SAS: 73.810% ± 10.754; week-2: 53.846% ± 11.886, $P = 0.003$) and the week-3 saline group (week-3 SAS%: 73.810 ± 10.754; week-3 saline: 51.020% ± 16.198, $P = 0.014$) (Figure 3b).

Looking more closely to the changes occurring within individual mice, we found that 6/7 mice in the saline treated group had increased seizure burdens between week 1 and week 3 and 1 mouse did not exhibit any change in seizure frequency from week 1 to week 3. Utilizing the same analysis in the group treated with SAS, the upward trend in seizure frequency found within the saline group was disrupted in the SAS group (Figure 3c). Lastly, 1 week of SAS or saline injections did not significantly alter the seizure duration (baseline: 45.317 ± 9.790 seconds; week-3 SAS: 48.636 ± 7.990 seconds; week-3 saline: 45.500 ± 11.528 seconds, $P = 0.220$) or seizure severity score (baseline: 3.704 ± 0.629; week-3 SAS: 3.800 ± 0.805; week-3 saline: 3.810 ± 0.512, $P = 0.464$) (Figure 3d).

Reduction in seizure frequency is due to acute effects of SAS

Knowing that the half-life of SAS in mice is estimated to be around 90 minutes[153], we next set out to analyze the temporal profile of the anti-seizure effects of SAS. The twice daily SAS or saline injections were given between 8-10am and 4-6pm every day throughout the treatment week. Given the short half-life of SAS and injections that only occurred during the day, we separated our seizure data into two groups, the seizures that occurred during the 12-hour light cycle, "day", and those that occurred during the 12-hour "night" cycle (Figure 4).

Plotting the cumulative seizure burden during the day and night, we found that SAS treatment had a clear effect during the day (Figure 4a, left) compared to the effects at night (Figure 4a, right). Indeed, there was a significant decrease in seizure frequency between the SAS and saline group (week-3 SAS: 0.016 ± 0.015; week-3 saline: 0.053 ± 0.028 seizures/hour, P = 0.015) (Figure 4b). However, during the night the seizure frequency of the SAS and saline group were almost identical (week-3 SAS: 0.0465 ± 0.039; week-3 saline: 0.0474 ± 0.031, P = 0.964) (Figure 4c). Despite similar seizure frequencies, only the saline group showed a significant increase in seizure frequency from week 1 to week 3 during the night (week-1 baseline: 0.021 ± 0.015; week-3 saline: 0.0474 ± 0.031, P = 0.018). This may be due to the higher variance of seizure frequencies seen in the SAS group (week-1 baseline: 0.021 ± 0.015; week-3 SAS: 0.0465 ± 0.040, P = 0.054).

Additionally, as EEG roughly surveys the electrical activity of neurons near the implanted electrodes, we investigated whether the effects of SAS could be captured on EEG via a reduction in EEG activity. Using a spectrogram to analyze the recorded EEG power 2 hours immediately preceding injection with SAS or saline and the EEG power 2 hours immediately post injection, we found an appreciable reduction in EEG activity from B1KOs following SAS injection compared to when given saline (Figure 5a). In order to quantify the change in EEG

activity with treatment we calculated the ratio of EEG power after injection divided by the EEG power before injection and compared these values between our groups. Therefore, a ratio of 1 would represent no change and a ratio below 1 would represent a decrease in EEG power after injection. As expected, we found that SAS treatment resulted in a significant reduction in the EEG power ratio compared to B1KOs that received saline (B1KO + saline: 1.044 ± 0.263; B1KO + SAS: 0.614 ± 0.307, $P = 0.034$) (Figure 5b). Surprisingly, among non-epileptic control mice there was no significant difference in the EEG power ratio between control mice that received SAS and those that received saline (Control + saline: 0.926 ± 0.144; Control + SAS: 1.017 ± 0.269, $P = 0.581$) (Figure 5b).

B1KO - xCT$^{-/-}$ double knockout cortical neurons are significantly hyperpolarized compared to B1KO – xCT$^{+/+}$

One important consideration in the investigation of SAS as a potential AED are the biological effects of SAS in addition to its ability to inhibit SXC. In its clinical use for the treatment of inflammatory bowel disease and rheumatoid arthritis sulfasalazine broadly acts as an anti-inflammatory drug and immunomodulator through inhibition of nuclear factor kappa B[154,155]. Due to these off-target effects, we set out to determine whether loss of function of SXC was also sufficient in decreasing hyperexcitability in B1KOs. Thus, we crossed our B1KO mouse line with a xCT$^{-/-}$ mouse line using xCT$^{-/-}$ breeders descendant from the strain originally described by Sato et al. 2005[156]. In this manner we were able to generate B1KO - xCT$^{-/-}$ double knockouts and examine their electrophysiological properties using acute brain slices. The following sets of experiments were repeated in 4 groups representing epileptic mice with SXC (B1KO – xCT$^{+/+}$) and without SXC (B1KO - xCT$^{-/-}$) and non-epileptic mice with SXC (Control - xCT$^{+/+}$) and without SXC (Control - xCT$^{-/-}$).

First, we examined the resting membrane potentials of layer 2/3 cortical pyramidal neurons from each of our groups and found that Control – $xCT^{-/-}$ neurons were significantly hyperpolarized compared to all other groups (Figure 6a). Interestingly, the three other groups all had similar resting membrane potentials (Control – $xCT^{-/-}$: -76.083 ± 3.105; Control – $xCT^{+/+}$: -71.857 ± 2.982; B1KO – $xCT^{-/-}$: -71.063 ± 3.110; B1KO – $xCT^{+/+}$: -71.000 ± 2.160). Next, we compared the threshold current needed to fire an action potential and found that Control - $xCT^{-/-}$ neurons required significantly more current to fire the first action potential compared to all other groups (Figure 6b). Once again, all the other groups behaved similarly (Control – $xCT^{-/-}$: 384.667 ± 123.357; Control – $xCT^{+/+}$: 236.286 ± 92.890; B1KO – $xCT^{-/-}$: 171.750 ± 56.259; B1KO – $xCT^{+/+}$: -157.143 ± 34.407). Our last experiment compared the number of action potentials elicited in serially increasing current injections among all groups. When comparing Controls with and without SXC we found that between 100 – 200 pA current injections, Control – $xCT^{-/-}$ neurons responded with significantly less action potentials (Figure 6c). Excitingly, between 160 – 240 pA current injections B1KO – $xCT^{-/-}$ neurons fired significantly less action potentials than B1KO – $xCT^{+/+}$ neurons, suggesting that knocking out SXC makes these B1KOs less hyperexcitable in high current environments (Figure 6d). In agreement with the previous results, Control - $xCT^{-/-}$ neurons fired significantly less action potentials compared to all other groups from 80 – 240pA current injections (Figure 6e).

Discussion

First, we report that 100% of B1KOs that were monitored via 24/7 video-EEG developed spontaneous recurrent seizures between 7 to 12 weeks of age. This is of particular importance in epilepsy research considering the mortality rate of chemoconvulsant status epilepticus models such as the use of pilocarpine. A study analyzing all of the pilocarpine induced status epilepticus

statistics from one lab (2413 total mice) found that only 33.5% of mice that received pilocarpine developed status epilepticus and survived to develop epilepsy[157]. Thus, comparatively the B1KO model is an effective and efficient model that can be used to reduce the number of mice needed to perform studies on the epileptogenic effects of chronic astrogliosis.

Previously our lab found that aggressive glioblastomas express high levels of SXC, and that this tumor associated epilepsy was susceptible to SXC inhibition via SAS[5-7].Additionally, a recent study using the self-sustained status epilepticus and pilocarpine epilepsy models found that $xCT^{-/-}$ mice had delayed epileptogenesis and a lower seizure burden compared to controls[56]. Our results agree with these previous studies as we found that inhibition of SXC, via SAS, was able to significantly reduce the seizure burden in B1KOs. Additionally, the anti-seizure effects of daily SAS treatment in our study were acute and did not affect seizure susceptibility throughout the night. This is most likely due to the known short half-life of SAS in mice and suggests that daily SAS treatment may not result in permanent anti-epileptic changes. However, in the current study we did not evaluate the long-term effects of daily SAS treatment beyond our 1-week treatment.

When evaluating the acute effects of SAS on EEG power we found that in epileptic mice there was a significant reduction in EEG power within 2 hours of SAS administration. Interestingly, in non-epileptic mice that received SAS there was no effect on EEG power. This may suggest that chronic astrogliosis increases SXC activity in an epileptic brain and that this increase in SXC activity is susceptible to inhibition compared to a healthy control. Of note, previous studies using human epileptic tissue[24] and mouse models of epilepsy[56] have reported significantly higher levels of SXC protein within epileptic tissue.

Knowing that SAS has biological effects beyond SXC inhibition, we crossed our B1KO mouse line with a $xCT^{-/-}$ mouse line to generate B1KO - $xCT^{-/-}$ double knockouts to evaluate the effects of complete SXC inhibition in the setting of chronic astrogliosis without the off-target effects associated with SAS. In summary, we found that non-epileptic mice lacking functional SXC had a hyperpolarized resting membrane potential compared to all other groups. Additionally, pyramidal neurons from non-epileptic mice without SXC required significantly higher current injections to fire their first action potential compared to all other groups. Lastly, in experiments evaluating the response of neurons to increasing current injections, we found that epileptic mice lacking SXC fired significantly less action potentials than epileptic mice with functional SXC between 160 and 240pA current injections.

Previously, we found that SAS preferentially decreased NMDA receptor mediated excitatory post synaptic currents (EPSCs) and had no effect on AMPA receptor mediated EPSCs[55]. Thus, we propose that in the setting of chronic astrogliosis SXC inhibition, via SAS, results in decreased extracellular glutamate which can lead to a decrease in neuronal NMDA receptor mediated inward currents and ultimately decreased neuronal hyperexcitability and reduction of seizures. In the current study we used SAS to inhibit SXC based on its FDA-approved status and known safety profile. However, we believe the ideal SXC inhibitor for the treatment of epilepsy should have limited off-target effects and a longer half-life. Based on the current findings and previous studies from our lab and others, we believe that further characterization of SXC inhibition for the treatment of epilepsy is warranted and promising.

Figures

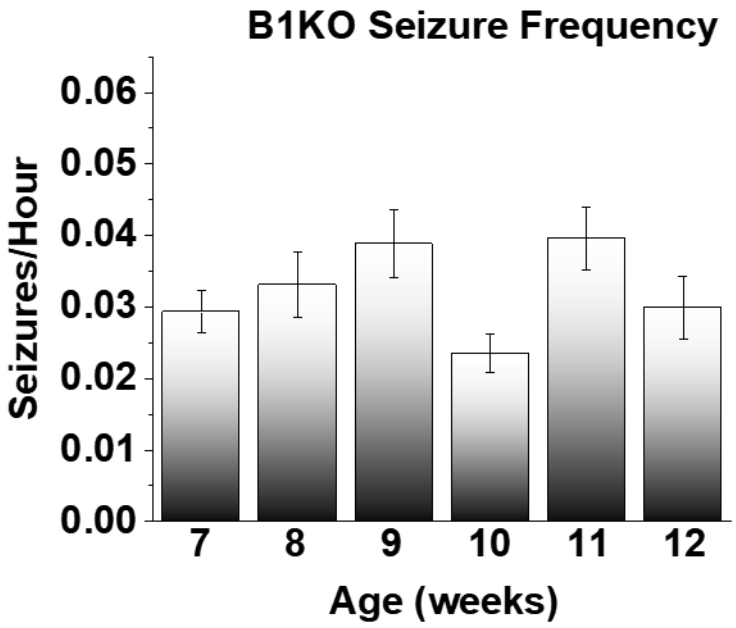

Figure 1: B1KO seizure burden between 7 – 12 weeks of age. The weekly seizure burden of B1KOs between 7 – 12 weeks of age was monitored via 24/7 video-EEG in 2 – 3-week increments. Units are in seizures/hour. Week 7: n=4, 0.029 ± 0.006. Week 8: n=13, 0.033 ± 0.016. Week 9: n=10, 0.039 ± 0.015. Week 10: n=12, 0.023 ± 0.009. Week 11: n=10, 0.040 ± 0.014. Week 12: n=8, 0.030 ± 0.013.

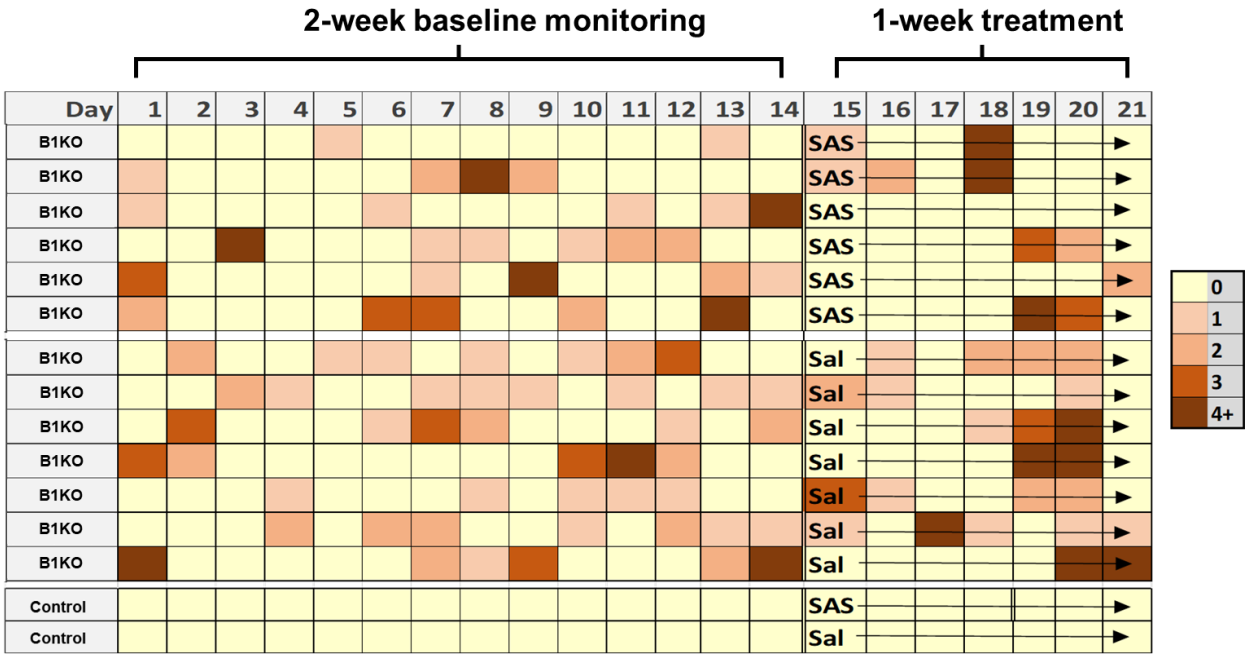

Figure 2: Heatmap of all seizures throughout the three-week experiment. This heatmap demonstrates the daily distribution of seizures over three weeks of 24/7 video-EEG. The top six rows represent the B1KOs that received SAS during the treatment week. The next seven rows represent the B1KOs that received saline during the treatment week. The last two rows are representative for the control mice that received SAS (n=4) or saline (n=7). No seizures were observed in any of the control mice.

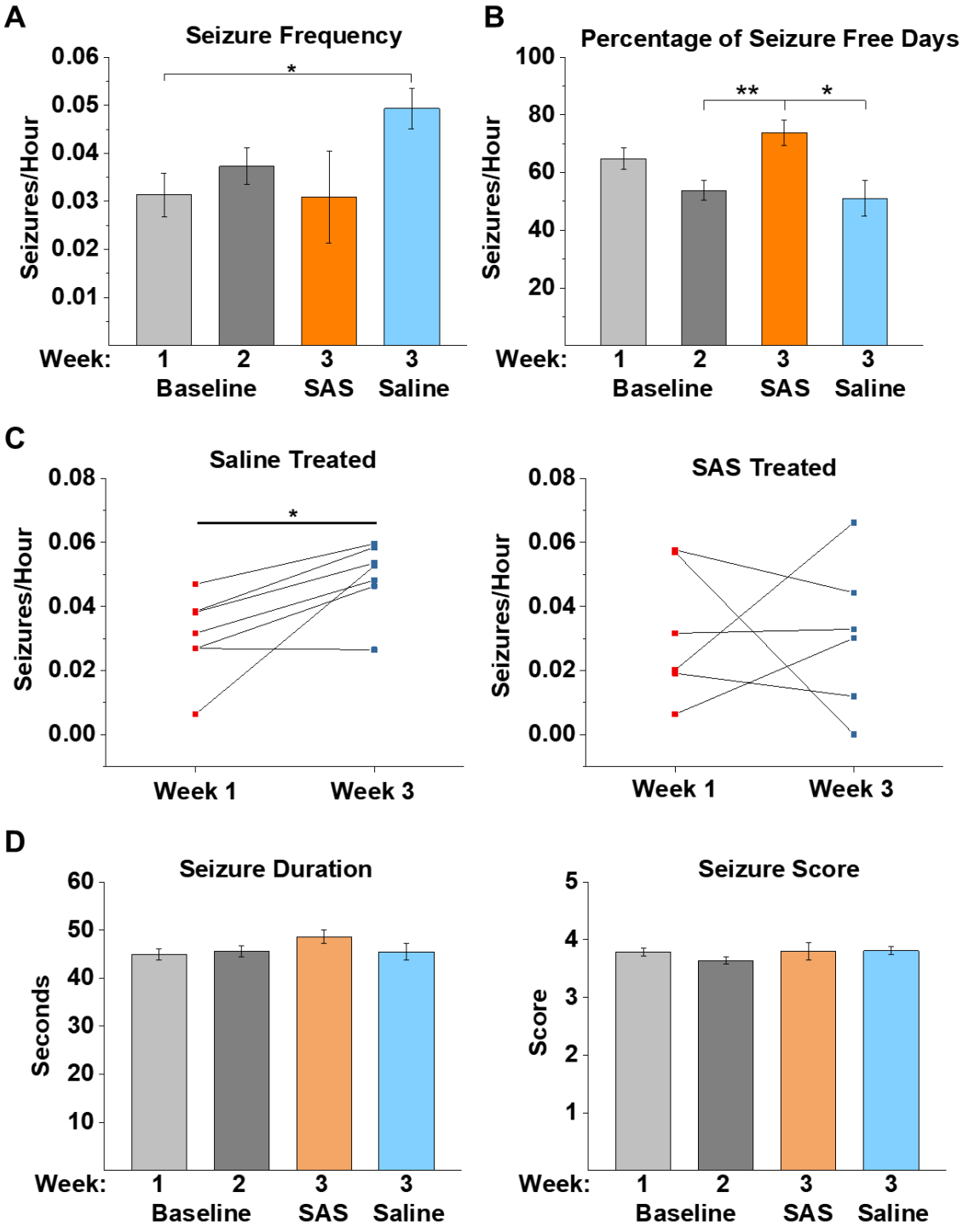

Figure 3: Seizure burden characteristics among all groups. (A) Comparison of weekly seizure frequency between baseline (weeks 1 and 2, n=13) and treatment groups (week 3-SAS, n=6 and week 3-saline, n=7). Seizure burden significantly increased between week 1 and week 3

of B1KOs that received saline treatment. (B) Percentage of seizure free days between baseline (weeks 1 and 2) and treatment groups (week 3-SAS and week 3-saline). B1KOs that received SAS during week 3 had a significantly higher percentage of seizure free days than week 2 or week 3-saline. (C) Tracking the change in individual seizure burden between B1KOs that eventually received saline (left) or SAS (right). SAS treatment prevented the significant increase in seizure frequency seen in B1KOs treated with saline. (D) Treatment with SAS or saline did not have an effect on the duration (left) or severity (right) of seizures.

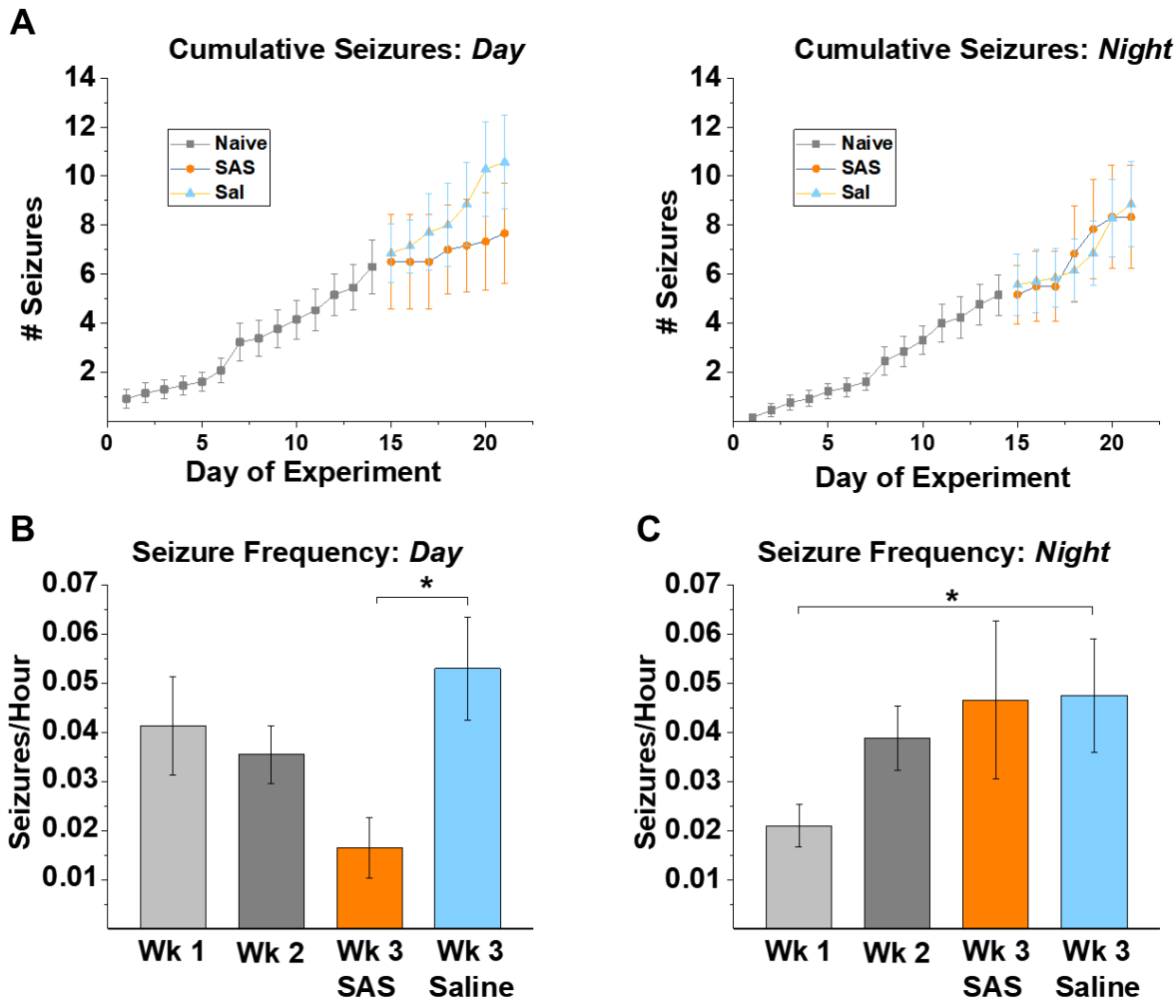

Figure 4: Seizure burden during the day and night. (A) Cumulative seizure burden throughout the experiment during the day (left) and night (right). (B) Weekly seizure burden during the day. B1KOs treated with SAS had significantly less seizures compared to the saline group during the day. (C) Weekly seizure burden during the night. B1KOs treated with saline had significantly more seizures compared to the week 1 seizure burden at night.

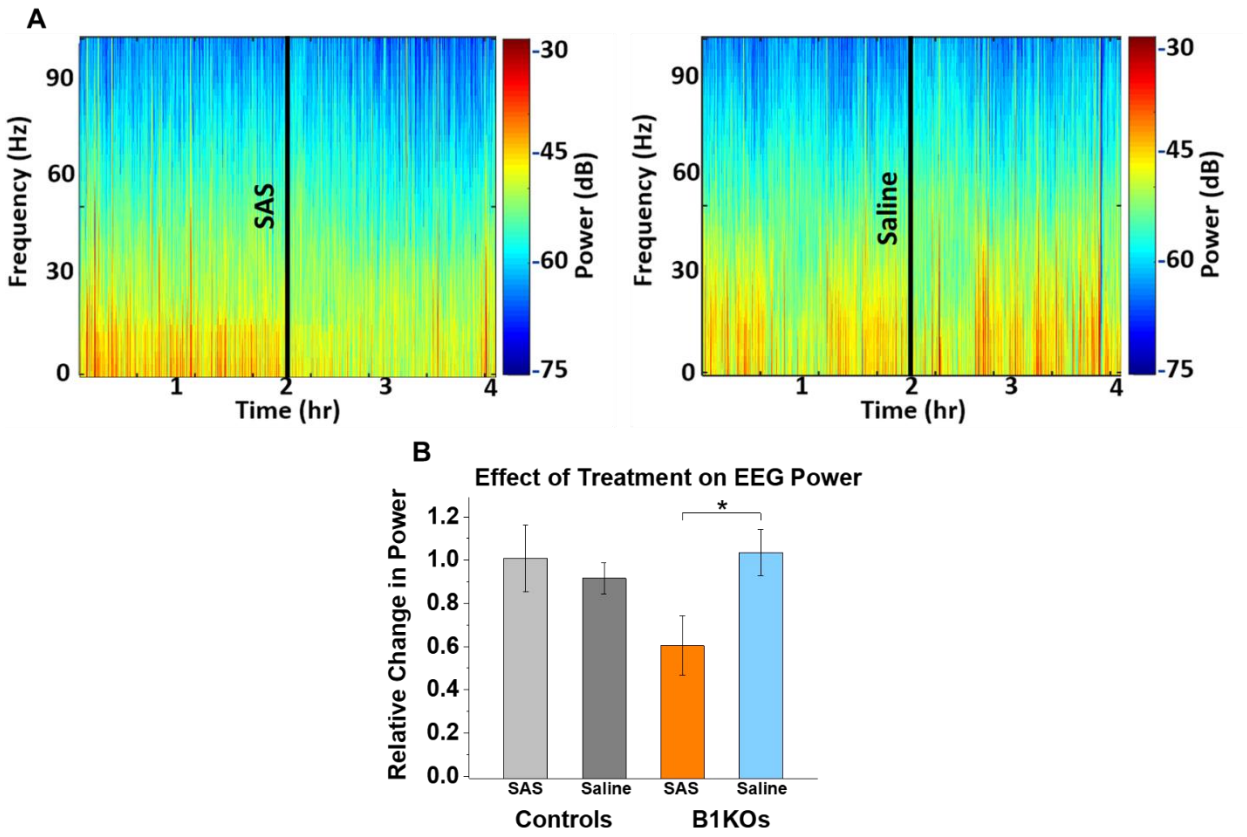

Figure 5: Acute effects of SAS and saline injections on EEG power in B1KOs and controls. (A) Representative spectrograms showing the change in EEG power of a B1KO two hours immediately preceding (0 – 2hrs) and two hours immediately after (2 – 4hrs) injection with either SAS (left) or saline (right). (B) Quantification of the relative change in power after SAS or saline injections in controls and B1KOs. Among B1KOs, SAS caused a significant decrease in relative power compared to the saline group. No significant change was observed in the control groups.

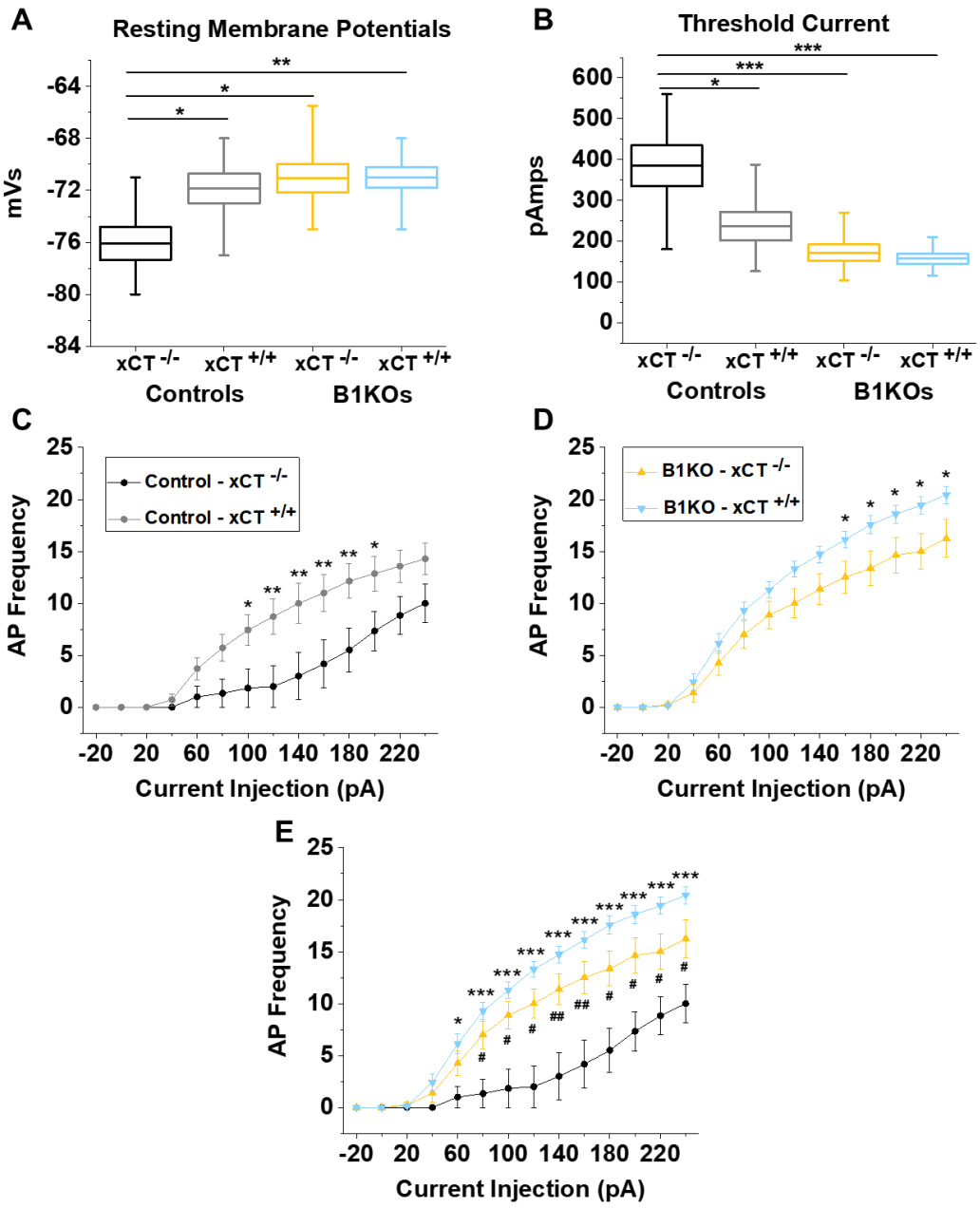

Figure 6: Electrophysiological properties of layer 2/3 cortical pyramidal neurons from B1KO-xCT$^{-/-}$ cross. (A) Resting membrane potentials of Control – xCT $^{-/-}$ neurons were found to be significantly hyperpolarized compared to all other groups. Control – xCT$^{-/-}$ (n=6) : -76.083 ± 3.105; Control – xCT$^{+/+}$ (n=7) : -71.857 ± 2.982; B1KO – xCT$^{-/-}$ (n=8) : -71.063 ± 3.110; B1KO – xCT$^{+/+}$ (n=7) : -71.000 ± 2.160. * P < 0.05, ** P < 0.01 (B) Control – xCT $^{-/-}$ neurons required significantly more current to fire an action potential compared to all other groups. Control – xCT$^{-/-}$ (n=6): 384.667 ± 123.357; Control – xCT$^{+/+}$ (n=7): 236.286 ± 92.890; B1KO – xCT$^{-/-}$ (n=8): 171.750 ± 56.259; B1KO – xCT$^{+/+}$ (n=7): -157.143 ± 34.407. * P < 0.05, *** P < 0.001 (C) Control – xCT $^{-/-}$ (n=6) neurons were found to fire significantly less action potentials from 100 – 200 pA current injections compared to Control – xCT$^{+/+}$ (n=7). * P < 0.05, ** P < 0.01. (D)

B1KO – xCT$^{-/-}$ (n=8) neurons fired significantly less action potentials from 160 -240 pAs compared to B1KO – xCT$^{+/+}$ (n=7). * $P < 0.05$. (E) Control – xCT $^{-/-}$ neurons fired significantly less action potentials than all other groups from 80 – 240 pAs. */# $P < 0.05$, ## $P < 0.001$, *** $P < 0.0001$

Chapter 5

Summary & Conclusion

Summary and future direction

Several animal models have been established and used to perform mechanistic studies on the pathophysiology of epilepsy over the past few decades[150]. Investigations using these models have led to the successful development of three generations of AEDs that continue to provide safe and efficacious treatment to individuals living with epilepsy[148]. Unfortunately, despite over 50 years of drug development, current AEDs continue to be ineffective in 1-in-3 epileptic patients[2,15,28]. Thus, a central motivation and objective of this dissertation was to broaden the search for novel AED targets that may help this patient population in need. Towards this end, the studies presented expand on previous research from our lab investigating the role of astrocytic SXC in the genesis and maintenance of acquired epilepsies. Additionally, we further characterize the novel B1KO epilepsy model that can be used to study the isolated effects of chronic astrogliosis in the development of epilepsy, in addition to, reporting the anti-seizure effects of SXC inhibition via SAS.

The foundational knowledge of this dissertation comes from investigations in the behavior and invasive mechanisms of aggressive glioblastomas. Prior work characterized altered glutamate transporter expression in gliomas as a crucial mediator of increased peritumoral glutamate levels[20-22]. A combination of decreased glutamate uptake, via altered GLT-1 and GLAST expression, and increased glutamate release, via SXC, was found to significantly contribute to neuronal hyperexcitability and tumor-associated epilepsy in mice implanted with human glioblastomas. Follow-up studies revealed that these aggressive glioblastomas were susceptible to SXC inhibition, using SAS, leading to inhibited tumor growth and a decrease in tumor-associated epileptiform activity [5,7]. Although other forms of acquired epilepsy do not have a concentration of mutated cells that highly express SXC, studies using human epileptic tissue

and chemoconvulsant mouse models of epilepsy have revealed that epileptic tissue expressed higher levels of SXC compared to health tissue[24,56]. Using these insights, we investigated whether similar processes may be involved in other forms of acquired epilepsy and whether SXC inhibition can alleviate seizure burden beyond tumor-associated epilepsies.

First, we investigated the efficacy of SXC inhibition in reducing neuronal hyperexcitability in a setting beyond glioblastomas. Utilizing acute brain slices and whole-cell patch clamp recordings we explored the ability of SXC inhibition to reduce epileptiform events using multiple, distinct pharmacological hyperexcitability models *ex vivo*[55]. We found that SAS was able to significantly decrease eEPSCs and that this was mediated via a specific reduction in NMDAR-mediated currents, while AMPAR-mediated currents were unaffected. Additionally, SAS was found to significantly decrease hyperexcitability in all models tested and completely blocked 4-AP induced epileptiform activity. Using voltage sensitive dyes, we found that SAS was able to reduce the amplitude of induced hyperexcitability in all models and the spread of evoked activity in all but one condition. Additionally, we found that co-application of a clinically used AED, topiramate, and SAS led to a synergistic reduction of epileptiform activity compared to the effects of topiramate alone.

After identifying the potential of SXC inhibition to reduce hyperexcitability using *ex vivo* models, we next wished to investigate whether SXC inhibition could decrease seizure burden *in vivo*. With the limitations of widely used mouse models of epilepsy in mind, we used the B1KO epilepsy model, which is characterized by widespread, chronic astrogliosis leading to spontaneous, recurrent seizures. In this manner we were able to investigate the isolated contributions of chronic astrogliosis to epileptogenesis, in the absence of confounding factors

such as neuronal death from excitotoxicity, systemic inflammation and loss of blood brain barrier function seen in other models of epilepsy.

First, we confirmed that 100% of monitored B1KOs developed spontaneous, recurrent seizures between 7 – 12 weeks of age. Within this age range naive B1KOs were found to have a seizure burden between 0.029 – 0.040 seizures/hour. Notably, the seizure burden among B1KOs was remarkably similar between litters compared to my experience with the pilocarpine model, in which the weekly seizure burden among groups of mice 4-weeks post SE ranged from ~0.02 – 0.30 seizures/hour (unpublished). Additionally, we observed that B1KOs rarely have more than 2-3 days of consecutive seizures but appear to have "seizure clusters", which is a phenomenon associated with medically refractory epilepsy among human epilepsies[151,152].

To test the efficacy of SAS as an AED in B1KOs, we monitored mice for a 2-week baseline period followed by a 1-week treatment period in which B1KOs received twice-daily intraperitoneal injections of either SAS or saline sham injection. We found that SAS prevented a significant increase in seizure burden seen in B1KOs that received sham saline injections. Additionally, we found that SAS significantly decrease seizure burden acutely during the day, when SAS was being administered. However, at night when SAS was systemically cleared, the seizure burden of B1KOs receiving SAS was almost identical to those receiving saline. Lastly, we generated a B1KO - $xCT^{-/-}$ mouse line to probe the electrophysiological properties of B1KO cortical pyramidal neurons with and without functional SXC. Using whole-cell patch clamp recordings we found that non-epileptic mice lacking functional SXC exhibited hyperpolarized pyramidal neurons. Additionally, B1KO - $xCT^{-/-}$ double knockouts were significantly less hyperexcitable compared to B1KO with functional SXC in their responses to serially increasing current injections.

An unfinished aspect of this project that future experiments could expand on involves zeroing in on the precise anti-seizure mechanisms that SXC inhibition mediates. Although the effects of SXC inhibition on extracellular glutamate levels has been investigated using *in vitro* glutamate assays and *in vivo* microdialysis, these techniques are unable to quantify and characterize changes occurring *in-situ*. iGluSnFR, is an exciting new glutamate sensor that allows investigators to visualize real-time changes in extracellular glutamate in culture, acute slice or *in vivo*. When expressed on membranes, iGluSnFR can bind to extracellular glutamate leading to a conformational shift exposing GFP-fluorescence. Expression of iGluSnFR is mediated using an AAV vector and multiple variants exist to selectively express this sensor in neurons or astrocytes. Use of this technique could lead to insights regarding the *in-situ* dynamics of SXC inhibition on extracellular glutamate.

Furthermore, investigations utilizing the B1KO - $xCT^{-/-}$ mouse line and electrophysiology could also help pinpoint and verify the mechanisms behind the anti-seizure effects of SXC inhibition. In Chapter 3 we found that SAS preferentially decreased evoked NMDAR-mediated currents in acute brain slices from healthy control mice. These results suggest that SXC inhibition leads to lower extracellular glutamate and lower activation of extrasynaptic NMDARs. Using the B1KO- $xCT^{-/-}$ line and electrophysiology we could investigate whether B1KO-$xCT^{+/+}$ mice have altered NMDAR-mediated currents and use the double knockouts to test whether these NMDAR-mediated currents are indeed decreased in B1KOs lacking SXC. Additionally, in Chapter 4 we found evidence that B1KO - $xCT^{-/-}$ mice fired significantly less action potentials in response to high current injections compared to B1KO-$xCT^{+/+}$ mice. An interesting follow-up experiment could determine if bath application of SAS is able to decrease the response of B1KO-$xCT^{+/+}$ mice to current injections to a level similar to B1KO - $xCT^{-/-}$. The proposed experiments

would improve our understanding of the effects of SXC inhibition and the effects of modulating ambient, extracellular glutamate levels.

Conclusion

It is well-appreciated that an imbalance between excitatory and inhibitory neurotransmission causes hyperexcitability in neuronal circuitry and underlies the generation of seizures and epileptogenesis. In order to devise effective strategies to help find relief for 1-in-3 epileptic patients who experience drug-resistant epilepsy we must continue to explore and understand the mechanisms regulating glutamate homeostasis in both physiological and pathological states. Towards this end, this dissertation explored the efficacy of targeting an astrocytic glutamate antiporter, SXC, as a novel AED target and further characterized a unique mouse model in which chronic astrogliosis is sufficient to induce spontaneous seizures and epilepsy.

The studies enclosed support the notion that astrocytes are uniquely positioned to act as a master regulator of glutamate within the CNS, and when dysregulated, can mediate pro-epileptic changes leading to seizure generation. We propose that inhibition of astrocytic SXC causes a decrease in ambient, extracellular glutamate that results in decreased activation of extrasynaptic NMDARs, ultimately leading to suppression of neuronal NMDAR-mediated slow inward currents. Although there are intrinsic challenges in ubiquitously targeting glutamatergic processes in the CNS, it has become increasingly evident that astrocytes can provide promising non-neuronal targets for regulating elevated levels of extracellular glutamate commonly seen with epilepsy. My hope is that this work can continue to be built upon and lead to the development of more specific and long-lasting SXC inhibitors for the treatment of epilepsy.

References

1. WHO: Epilepsy Fact Sheet. 2018; http://www.who.int/news-room/fact-sheets/detail/epilepsy.

2. Brodie MJ, Barry SJ, Bamagous GA, Norrie JD, Kwan P. Patterns of treatment response in newly diagnosed epilepsy. Neurology. 2012;78(20):1548-1554.

3. DA B, ZX X, H S, CJ S, PW K. The origin and neuronal function of in vivo nonsynaptic glutamate. The Journal of neuroscience : the official journal of the Society for Neuroscience. 2002;22(20).

4. AL L, SM OD, MT S-O, et al. Contrasting the Role of xCT and GLT-1 Upregulation in the Ability of Ceftriaxone to Attenuate the Cue-Induced Reinstatement of Cocaine Seeking and Normalize AMPA Receptor Subunit Expression. The Journal of neuroscience : the official journal of the Society for Neuroscience. 2017;37(24).

5. Buckingham SC, Campbell SL, Haas BR, et al. Glutamate release by primary brain tumors induces epileptic activity. Nat Med. 2011;17(10):1269-1274.

6. Campbell SL, Buckingham SC, Sontheimer H. Human glioma cells induce hyperexcitability in cortical networks. Epilepsia. 2012;53(8):1360-1370.

7. Robert SM, Buckingham SC, Campbell SL, et al. SLC7A11 expression is associated with seizures and predicts poor survival in patients with malignant glioma. Sci Transl Med. 2015;7(289):289ra286.

8. Epilepsies IoMUCotPHDot. Epilepsy Across the Spectrum: Promoting Health and Understanding2012.

9. Fisher RS, Acevedo C, Arzimanoglou A, et al. ILAE official report: a practical clinical definition of epilepsy. Epilepsia. 2014;55(4):475-482.

10. Fisher RS, Cross JH, French JA, et al. Operational classification of seizure types by the International League Against Epilepsy: Position Paper of the ILAE Commission for Classification and Terminology. Epilepsia. 2017;58(4):522-530.

11. Jobst BC, Cascino GD. Resective epilepsy surgery for drug-resistant focal epilepsy: a review. JAMA. 2015;313(3):285-293.

12. Rogawski MA, Löscher W. The neurobiology of antiepileptic drugs. Nat Rev Neurosci. 2004;5(7):553-564.

13. Schmidt D, Löscher W. Drug resistance in epilepsy: putative neurobiologic and clinical mechanisms. Epilepsia. 2005;46(6):858-877.

14. Kwan P, Schachter SC, Brodie MJ. Drug-resistant epilepsy. N Engl J Med. 2011;365(10):919-926.

15. Coatsworth JJ. Studies on the clinical efficacy of marketed antiepileptic drugs. Bethesda, Md.: Bethesda, Md., National Institutes of Health

for sale by the Supt. of Docs., U.S. Govt. Print. Off., Washington; 1971.

16. Bannai S, Kitamura E. Transport interaction of L-cystine and L-glutamate in human diploid fibroblasts in culture. J Biol Chem. 1980;255(6):2372-2376.

17. Bannai S, Kitamura E. Role of proton dissociation in the transport of cystine and glutamate in human diploid fibroblasts in culture. J Biol Chem. 1981;256(11):5770-5772.

18. Sagara J, Miura K, Bannai S. Cystine uptake and glutathione level in fetal brain cells in primary culture and in suspension. J Neurochem. 1993;61(5):1667-1671.

19. Sato H, Tamba M, Ishii T, Bannai S. Cloning and expression of a plasma membrane cystine/glutamate exchange transporter composed of two distinct proteins. J Biol Chem. 1999;274(17):11455-11458.
20. Ye ZC, Rothstein JD, Sontheimer H. Compromised glutamate transport in human glioma cells: reduction-mislocalization of sodium-dependent glutamate transporters and enhanced activity of cystine-glutamate exchange. J Neurosci. 1999;19(24):10767-10777.
21. Chung WJ, Lyons SA, Nelson GM, et al. Inhibition of cystine uptake disrupts the growth of primary brain tumors. J Neurosci. 2005;25(31):7101-7110.
22. Chung WJ, Sontheimer H. Sulfasalazine inhibits the growth of primary brain tumors independent of nuclear factor-kappaB. J Neurochem. 2009;110(1):182-193.
23. S O-H, QX H, VV F-A, et al. The cystine-glutamate exchanger (xCT, Slc7a11) is expressed in significant concentrations in a subpopulation of astrocytes in the mouse brain. Glia. 2018;66(5).
24. Lewerenz J, Baxter P, Kassubek R, et al. Phosphoinositide 3-kinases upregulate system xc(-) via eukaryotic initiation factor 2α and activating transcription factor 4 - A pathway active in glioblastomas and epilepsy. Antioxid Redox Signal. 2014;20(18):2907-2922.
25. K L, JV L, G A, et al. Anticonvulsant and antiepileptogenic effects of system [Formula: see text] inactivation in chronic epilepsy models. Epilepsia. 2019;60(7).
26. Robel S, Mori T, Zoubaa S, et al. Conditional deletion of beta1-integrin in astroglia causes partial reactive gliosis. Glia. 2009;57(15):1630-1647.
27. Robel S, Buckingham SC, Boni JL, et al. Reactive astrogliosis causes the development of spontaneous seizures. J Neurosci. 2015;35(8):3330-3345.
28. W L, D S. Modern antiepileptic drug development has failed to deliver: ways out of the current dilemma. Epilepsia. 2011;52(4).
29. McKenna MC. Glutamate pays its own way in astrocytes. Front Endocrinol (Lausanne). 2013;4:191.
30. Hawkins RA. The blood-brain barrier and glutamate. Am J Clin Nutr. 2009;90(3):867S-874S.
31. A V, M N. Physiology of Astroglia. Physiological reviews. 2018;98(1).
32. L H, R D, A S, SR R. Astrocytes: glutamate producers for neurons. Journal of neuroscience research. 1999;57(4).
33. Anlauf E, Derouiche A. Glutamine synthetase as an astrocytic marker: its cell type and vesicle localization. Front Endocrinol (Lausanne). 2013;4:144.
34. Zhu H, Wang N, Yao L, et al. Moderate UV Exposure Enhances Learning and Memory by Promoting a Novel Glutamate Biosynthetic Pathway in the Brain. Cell. 2018;173(7):1716-1727.e1717.
35. Schousboe A, Scafidi S, Bak LK, Waagepetersen HS, McKenna MC. Glutamate metabolism in the brain focusing on astrocytes. Adv Neurobiol. 2014;11:13-30.
36. WS C, NJ A, C E. Astrocytes Control Synapse Formation, Function, and Elimination. Cold Spring Harbor perspectives in biology. 2015;7(9).
37. TR M, DK B, TA F. Turning down the volume: Astrocyte volume change in the generation and termination of epileptic seizures. Neurobiology of disease. 2017;104.
38. R C, A N, S H. ECS Dynamism and Its Influence on Neuronal Excitability and Seizures. Neurochemical research. 2019;44(5).

39. Nielsen S, Nagelhus EA, Amiry-Moghaddam M, Bourque C, Agre P, Ottersen OP. Specialized membrane domains for water transport in glial cells: high-resolution immunogold cytochemistry of aquaporin-4 in rat brain. J Neurosci. 1997;17(1):171-180.
40. J T, VVGK I, UV N. Super-Resolution Imaging of the Extracellular Space in Living Brain Tissue. Cell. 2018;172(5).
41. MJ D, DD S. Extracellular hippocampal glutamate and spontaneous seizure in the conscious human brain. Lancet (London, England). 1993;341(8861).
42. K L, T M, T T, D D, DK B, TA F. Osmotic Edema Rapidly Increases Neuronal Excitability Through Activation of NMDA Receptor-Dependent Slow Inward Currents in Juvenile and Adult Hippocampus. ASN neuro. 2015;7(5).
43. Binder DK, Papadopoulos MC, Haggie PM, Verkman AS. In vivo measurement of brain extracellular space diffusion by cortical surface photobleaching. J Neurosci. 2004;24(37):8049-8056.
44. DK B, K O, T M, AS V, GT M. Increased seizure threshold in mice lacking aquaporin-4 water channels. Neuroreport. 2004;15(2).
45. DK B, X Y, Z Z, TJ S, AS V, GT M. Increased seizure duration and slowed potassium kinetics in mice lacking aquaporin-4 water channels. Glia. 2006;53(6).
46. KA P, H S. Contribution of chloride channels to volume regulation of cortical astrocytes. American journal of physiology. Cell physiology. 2003;284(6).
47. KA P, H S. Biophysical and pharmacological characterization of hypotonically activated chloride currents in cortical astrocytes. Glia. 2004;46(4).
48. FK V, F U, J M, et al. Identification of LRRC8 heteromers as an essential component of the volume-regulated anion channel VRAC. Science (New York, N.Y.). 2014;344(6184).
49. Z Q, AE D, J M, et al. SWELL1, a plasma membrane protein, is an essential component of volume-regulated anion channel. Cell. 2014;157(2).
50. F F, E S, MG M, et al. LRRC8A is essential for swelling-activated chloride current and for regulatory volume decrease in astrocytes. FASEB journal : official publication of the Federation of American Societies for Experimental Biology. 2019;33(1).
51. J Y, MDC V, J C, J O-O, J C, Z Q. Glutamate-Releasing SWELL1 Channel in Astrocytes Modulates Synaptic Transmission and Promotes Brain Damage in Stroke. Neuron. 2019;102(4).
52. JJ Z, Y L, SR C, JY S, R S, HL P. LRRC8A-dependent volume-regulated anion channels contribute to ischemia-induced brain injury and glutamatergic input to hippocampal neurons. Experimental neurology. 2020;332.
53. Pál B. Involvement of extrasynaptic glutamate in physiological and pathophysiological changes of neuronal excitability. Cell Mol Life Sci. 2018;75(16):2917-2949.
54. De Bundel D, Schallier A, Loyens E, et al. Loss of system x(c)- does not induce oxidative stress but decreases extracellular glutamate in hippocampus and influences spatial working memory and limbic seizure susceptibility. J Neurosci. 2011;31(15):5792-5803.
55. Alcoreza O, Tewari BP, Bouslog A, Savoia A, Sontheimer H, Campbell SL. Sulfasalazine decreases mouse cortical hyperexcitability. Epilepsia. 2019;60(7):1365-1377.
56. Leclercq K, Liefferinge JV, Albertini G, et al. Anticonvulsant and antiepileptogenic effects of system. Epilepsia. 2019;60(7):1412-1423.
57. Sears SMS, Hewett JA, Hewett SJ. Decreased epileptogenesis in mice lacking the System x. Epilepsia Open. 2019;4(1):133-143.

58. JL L, G A, EJ D, et al. Genetic and pharmacological manipulation of glial glutamate transporters does not alter infection-induced seizure activity. Experimental neurology. 2019;318.
59. MF C, JE L, DC P, DJ D, RS F. Infiltrating macrophages are key to the development of seizures following virus infection. Journal of virology. 2013;87(3).
60. Patel DC, Wallis G, Dahle EJ, et al. Hippocampal TNFα Signaling Contributes to Seizure Generation in an Infection-Induced Mouse Model of Limbic Epilepsy. eNeuro. 2017;4(2):ENEURO.0105-0117.2017.
61. T P, J D, M T, JC F, PG H. Astrocytic control of synaptic function. Philosophical transactions of the Royal Society of London. Series B, Biological sciences. 2017;372(1715).
62. DC P, BP T, L C, H S. Neuron-glia interactions in the pathophysiology of epilepsy. Nature reviews. Neuroscience. 2019;20(5).
63. T F, O P, S G, T P, PG H, G C. Neuronal synchrony mediated by astrocytic glutamate through activation of extrasynaptic NMDA receptors. Neuron. 2004;43(5).
64. MC A, AS K, S C, E A. Glutamate released from glial cells synchronizes neuronal activity in the hippocampus. The Journal of neuroscience : the official journal of the Society for Neuroscience. 2004;24(31).
65. P P. Molecular basis of NMDA receptor functional diversity. The European journal of neuroscience. 2011;33(8).
66. FN S, A P-S, A M, et al. Extrasynaptic glutamate release through cystine/glutamate antiporter contributes to ischemic damage. The Journal of clinical investigation. 2014;124(8).
67. M G-G, T Z, LM R, P B, G C. Insights into the release mechanism of astrocytic glutamate evoking in neurons NMDA receptor-mediated slow depolarizing inward currents. Glia. 2018;66(10).
68. Featherstone DE, Shippy SA. Regulation of synaptic transmission by ambient extracellular glutamate. Neuroscientist. 2008;14(2):171-181.
69. A R, J L. Glutamatergic Signaling in the Central Nervous System: Ionotropic and Metabotropic Receptors in Concert. Neuron. 2018;98(6).
70. FM R, LB V, RG P, RP O, SS F. Metabotropic glutamate receptors and neurodegenerative diseases. Pharmacological research. 2017;115.
71. CM N, PJ C. Metabotropic glutamate receptors: physiology, pharmacology, and disease. Annual review of pharmacology and toxicology. 2010;50.
72. Z N, E M, P S, P S. Subsynaptic segregation of metabotropic and ionotropic glutamate receptors as revealed by immunogold localization. Neuroscience. 1994;61(3).
73. R L, JD R, R S, H O, P S. Differential plasma membrane distribution of metabotropic glutamate receptors mGluR1 alpha, mGluR2 and mGluR5, relative to neurotransmitter release sites. Journal of chemical neuroanatomy. 1997;13(4).
74. I B, AJ B, C K, et al. Temporal lobe epilepsy associated up-regulation of metabotropic glutamate receptors: correlated changes in mGluR1 mRNA and protein expression in experimental animals and human patients. Journal of neuropathology and experimental neurology. 2000;59(1).
75. V H, P M, XQ W, et al. Metabotropic glutamate receptor 1-induced upregulation of NMDA receptor current: mediation through the Pyk2/Src-family kinase pathway in cortical

neurons. The Journal of neuroscience : the official journal of the Society for Neuroscience. 2002;22(13).

76. Y W, Y K, S F, K T, T U, C K. Participation of metabotropic glutamate receptors in pentetrazol-induced kindled seizure. Epilepsia. 2011;52(1).

77. Sun W, McConnell E, Pare JF, et al. Glutamate-dependent neuroglial calcium signaling differs between young and adult brain. Science. 2013;339(6116):197-200.

78. AD U, PJ W, JA W, KS W. Conditional Knock-out of mGluR5 from Astrocytes during Epilepsy Development Impairs High-Frequency Glutamate Uptake. The Journal of neuroscience : the official journal of the Society for Neuroscience. 2019;39(4).

79. Kelly E, Schaeffer SM, Dhamne SC, et al. mGluR5 Modulation of Behavioral and Epileptic Phenotypes in a Mouse Model of Tuberous Sclerosis Complex. Neuropsychopharmacology. 2018;43(6):1457-1465.

80. S D, T F, Y Z, et al. Enhanced astrocytic Ca2+ signals contribute to neuronal excitotoxicity after status epilepticus. The Journal of neuroscience : the official journal of the Society for Neuroscience. 2007;27(40).

81. PJ C, JP P. Pharmacology and functions of metabotropic glutamate receptors. Annual review of pharmacology and toxicology. 1997;37.

82. PS P, C M. Presynaptic glutamate receptors: physiological functions and mechanisms of action. Nature reviews. Neuroscience. 2008;9(6).

83. C C, G B, G M, et al. The use of knock-out mice unravels distinct roles for mGlu2 and mGlu3 metabotropic glutamate receptors in mechanisms of neurodegeneration/neuroprotection. The Journal of neuroscience : the official journal of the Society for Neuroscience. 2007;27(31).

84. F N, J B, GL C, et al. Metabotropic glutamate receptors: from the workbench to the bedside. Neuropharmacology. 2011;60(7-8).

85. Di Menna L, Joffe ME, Iacovelli L, et al. Functional partnership between mGlu3 and mGlu5 metabotropic glutamate receptors in the central nervous system. Neuropharmacology. 2018;128:301-313.

86. LF PO, J C, R S, MM Z, ER GS. Abnormal mGluR2/3 expression in the perforant path termination zones and mossy fibers of chronically epileptic rats. Brain research. 2006;1098(1).

87. FR T, WL L, H G, Y C, YT L, SC C. Expression of different isoforms of protein kinase C in the rat hippocampus after pilocarpine-induced status epilepticus with special reference to CA1 area and the dentate gyrus. Hippocampus. 2004;14(1).

88. ER G-S, LF O, MF A, B H, S F, BS E. Impaired expression and function of group II metabotropic glutamate receptors in pilocarpine-treated chronically epileptic rats. Brain research. 2008;1240.

89. Tang FR, Lee WL, Gao H, Chen Y, Loh YT, Chia SC. Expression of different isoforms of protein kinase C in the rat hippocampus after pilocarpine-induced status epilepticus with special reference to CA1 area and the dentate gyrus. Hippocampus. 2004;14(1):87-98.

90. RX M, M J, A T, PM B, AG C, BS M. Anti-epileptic activity of group II metabotropic glutamate receptor agonists (--)-2-oxa-4-aminobicyclo[3.1.0]hexane-4,6-dicarboxylate (LY379268) and (--)-2-thia-4-aminobicyclo[3.1.0]hexane-4,6-dicarboxylate (LY389795). Neuropharmacology. 2001;41(1).

91. RT N, F B, S C, et al. The preferential mGlu2/3 receptor antagonist, LY341495, reduces the frequency of spike-wave discharges in the WAG/Rij rat model of absence epilepsy. Neuropharmacology. 2005;49 Suppl 1.
92. RT N, I S, F B, et al. Protective role for type-1 metabotropic glutamate receptors against spike and wave discharges in the WAG/Rij rat model of absence epilepsy. Neuropharmacology. 2011;60(7-8).
93. G M, A T-S, G C, Q C, DF C. Cellular localization of mGluR3 and mGluR5 mRNAs in normal and injured rat brain. Brain research. 2007;1149.
94. E A, EA vV, OA M, D T, FH dS, JA G. Upregulation of metabotropic glutamate receptor subtype mGluR3 and mGluR5 in reactive astrocytes in a rat model of mesial temporal lobe epilepsy. The European journal of neuroscience. 2000;12(7).
95. F F, C C, E V, S M, J X. Activated astrocytes in areas of kainate-induced neuronal injury upregulate the expression of the metabotropic glutamate receptors 2/3 and 5. Experimental brain research. 2001;137(1).
96. Aronica E, Gorter JA, Ijlst-Keizers H, et al. Expression and functional role of mGluR3 and mGluR5 in human astrocytes and glioma cells: opposite regulation of glutamate transporter proteins. Eur J Neurosci. 2003;17(10):2106-2118.
97. J L, J T, J M, M D, R W, Y W. Dynamic transition of neuronal firing induced by abnormal astrocytic glutamate oscillation. Scientific reports. 2016;6.
98. C DV, S M-S, E A, et al. Glia-neuron interactions underlie state transitions to generalized seizures. Nature communications. 2019;10(1).
99. Frampton JE. Perampanel: A Review in Drug-Resistant Epilepsy. Drugs. 2015;75(14):1657-1668.
100. Klein P, Friedman A, Hameed MQ, et al. Repurposed molecules for antiepileptogenesis: Missing an opportunity to prevent epilepsy? Epilepsia. 2020;61(3):359-386.
101. Rogawski MA, Löscher W, Rho JM. Mechanisms of Action of Antiseizure Drugs and the Ketogenic Diet. Cold Spring Harb Perspect Med. 2016;6(5).
102. Rosati A, De Masi S, Guerrini R. Ketamine for Refractory Status Epilepticus: A Systematic Review. CNS Drugs. 2018;32(11):997-1009.
103. Dooley DJ, Taylor CP, Donevan S, Feltner D. Ca2+ channel alpha2delta ligands: novel modulators of neurotransmission. Trends Pharmacol Sci. 2007;28(2):75-82.
104. Löscher W, Gillard M, Sands ZA, Kaminski RM, Klitgaard H. Synaptic Vesicle Glycoprotein 2A Ligands in the Treatment of Epilepsy and Beyond. CNS Drugs. 2016;30(11):1055-1077.
105. Yang X, Bognar J, He T, et al. Brivaracetam augments short-term depression and slows vesicle recycling. Epilepsia. 2015;56(12):1899-1909.
106. Sha L, Wang X, Li J, et al. Pharmacologic inhibition of Hsp90 to prevent GLT-1 degradation as an effective therapy for epilepsy. J Exp Med. 2017;214(2):547-563.
107. Goodrich GS, Kabakov AY, Hameed MQ, Dhamne SC, Rosenberg PA, Rotenberg A. Ceftriaxone treatment after traumatic brain injury restores expression of the glutamate transporter, GLT-1, reduces regional gliosis, and reduces post-traumatic seizures in the rat. J Neurotrauma. 2013;30(16):1434-1441.
108. Hameed MQ, Hsieh TH, Morales-Quezada L, et al. Ceftriaxone Treatment Preserves Cortical Inhibitory Interneuron Function via Transient Salvage of GLT-1 in a Rat Traumatic Brain Injury Model. Cereb Cortex. 2019;29(11):4506-4518.

109. Lewerenz J, Albrecht P, Tien ML, et al. Induction of Nrf2 and xCT are involved in the action of the neuroprotective antibiotic ceftriaxone in vitro. J Neurochem. 2009;111(2):332-343.
110. Kingston AE, Griffey K, Johnson MP, et al. Inhibition of group I metabotropic glutamate receptor responses in vivo in rats by a new generation of carboxyphenylglycine-like amino acid antagonists. Neurosci Lett. 2002;330(2):127-130.
111. Celli R, Santolini I, Van Luijtelaar G, Ngomba RT, Bruno V, Nicoletti F. Targeting metabotropic glutamate receptors in the treatment of epilepsy: rationale and current status. Expert Opin Ther Targets. 2019;23(4):341-351.
112. Álvarez-Ferradas C, Morales JC, Wellmann M, et al. Enhanced astroglial Ca2+ signaling increases excitatory synaptic strength in the epileptic brain. Glia. 2015;63(9):1507-1521.
113. Smolders I, Lindekens H, Clinckers R, et al. In vivo modulation of extracellular hippocampal glutamate and GABA levels and limbic seizures by group I and II metabotropic glutamate receptor ligands. J Neurochem. 2004;88(5):1068-1077.
114. Qian F, Tang FR. Metabotropic Glutamate Receptors and Interacting Proteins in Epileptogenesis. Curr Neuropharmacol. 2016;14(5):551-562.
115. Thomsen C, Klitgaard H, Sheardown M, et al. (S)-4-carboxy-3-hydroxyphenylglycine, an antagonist of metabotropic glutamate receptor (mGluR) 1a and an agonist of mGluR2, protects against audiogenic seizures in DBA/2 mice. J Neurochem. 1994;62(6):2492-2495.
116. Dalby NO, Thomsen C. Modulation of seizure activity in mice by metabotropic glutamate receptor ligands. J Pharmacol Exp Ther. 1996;276(2):516-522.
117. Attwell PJ, Singh Kent N, Jane DE, Croucher MJ, Bradford HF. Anticonvulsant and glutamate release-inhibiting properties of the highly potent metabotropic glutamate receptor agonist (2S,2'R, 3'R)-2-(2',3'-dicarboxycyclopropyl)glycine (DCG-IV). Brain Res. 1998;805(1-2):138-143.
118. Miyamoto M, Ishida M, Shinozaki H. Anticonvulsive and neuroprotective actions of a potent agonist (DCG-IV) for group II metabotropic glutamate receptors against intraventricular kainate in the rat. Neuroscience. 1997;77(1):131-140.
119. Metcalf CS, Klein BD, Smith MD, et al. Efficacy of mGlu. Epilepsia. 2017;58(3):484-493.
120. Metcalf CS, Klein BD, Smith MD, et al. Potent and selective pharmacodynamic synergy between the metabotropic glutamate receptor subtype 2-positive allosteric modulator JNJ-46356479 and levetiracetam in the mouse 6-Hz (44-mA) model. Epilepsia. 2018;59(3):724-735.
121. Devinsky O, Vezzani A, Najjar S, De Lanerolle NC, Rogawski MA. Glia and epilepsy: excitability and inflammation. Trends Neurosci. 2013;36(3):174-184.
122. Coulter DA, Steinhäuser C. Role of astrocytes in epilepsy. Cold Spring Harb Perspect Med. 2015;5(3):a022434.
123. Binder DK. Astrocytes: Stars of the Sacred Disease. Epilepsy Curr. 2018;18(3):172-179.
124. Massie A, Boillée S, Hewett S, Knackstedt L, Lewerenz J. Main path and byways: non-vesicular glutamate release by system xc(-) as an important modifier of glutamatergic neurotransmission. J Neurochem. 2015;135(6):1062-1079.
125. Bridges R, Lutgen V, Lobner D, Baker DA. Thinking outside the cleft to understand synaptic activity: contribution of the cystine-glutamate antiporter (System xc-) to normal and pathological glutamatergic signaling. Pharmacol Rev. 2012;64(3):780-802.
126. !!! INVALID CITATION !!! {}.

127. Kampa BM, Clements J, Jonas P, Stuart GJ. Kinetics of Mg2+ unblock of NMDA receptors: implications for spike-timing dependent synaptic plasticity. J Physiol. 2004;556(Pt 2):337-345.
128. Glauser T, Ben-Menachem E, Bourgeois B, et al. Updated ILAE evidence review of antiepileptic drug efficacy and effectiveness as initial monotherapy for epileptic seizures and syndromes. Epilepsia. 2013;54(3):551-563.
129. DeFazio RA, Hablitz JJ. Horizontal spread of activity in neocortical inhibitory networks. Brain Res Dev Brain Res. 2005;157(1):83-92.
130. Ryu BR, Lee YA, Won SJ, et al. The novel neuroprotective action of sulfasalazine through blockade of NMDA receptors. J Pharmacol Exp Ther. 2003;305(1):48-56.
131. Noh JH, Gwag BJ, Chung JM. Underlying mechanism for NMDA receptor antagonism by the anti-inflammatory drug, sulfasalazine, in mouse cortical neurons. Neuropharmacology. 2006;50(1):1-15.
132. Yuste R, Tank DW, Kleinfeld D. Functional study of the rat cortical microcircuitry with voltage-sensitive dye imaging of neocortical slices. Cereb Cortex. 1997;7(6):546-558.
133. Langenstroth M, Albowitz B, Kuhnt U. Partial suppression of GABAA-mediated inhibition induces spatially restricted epileptiform activity in guinea pig neocortical slices. Neurosci Lett. 1996;210(2):103-106.
134. D'Antuono M, Köhling R, Ricalzone S, Gotman J, Biagini G, Avoli M. Antiepileptic drugs abolish ictal but not interictal epileptiform discharges in vitro. Epilepsia. 2010;51(3):423-431.
135. Gotman J, Marciani MG. Electroencephalographic spiking activity, drug levels, and seizure occurrence in epileptic patients. Ann Neurol. 1985;17(6):597-603.
136. West PJ, Saunders GW, Billingsley P, et al. Recurrent epileptiform discharges in the medial entorhinal cortex of kainate-treated rats are differentially sensitive to antiseizure drugs. Epilepsia. 2018;59(11):2035-2048.
137. Hesdorffer DC, Logroscino G, Benn EK, Katri N, Cascino G, Hauser WA. Estimating risk for developing epilepsy: a population-based study in Rochester, Minnesota. Neurology. 2011;76(1):23-27.
138. Campos G, Fortuna A, Falcão A, Alves G. In vitro and in vivo experimental models employed in the discovery and development of antiepileptic drugs for pharmacoresistant epilepsy. Epilepsy Res. 2018;146:63-86.
139. Brodie MJ, Yuen AW. Lamotrigine substitution study: evidence for synergism with sodium valproate? 105 Study Group. Epilepsy Res. 1997;26(3):423-432.
140. Pisani F, Oteri G, Russo MF, Di Perri R, Perucca E, Richens A. The efficacy of valproate-lamotrigine comedication in refractory complex partial seizures: evidence for a pharmacodynamic interaction. Epilepsia. 1999;40(8):1141-1146.
141. Beyenburg S, Stavem K, Schmidt D. Placebo-corrected efficacy of modern antiepileptic drugs for refractory epilepsy: systematic review and meta-analysis. Epilepsia. 2010;51(1):7-26.
142. Vargas-Sánchez K, Mogilevskaya M, Rodríguez-Pérez J, Rubiano MG, Javela JJ, González-Reyes RE. Astroglial role in the pathophysiology of status. Oncotarget. 2018;9(42):26954-26976.
143. Eid T, Lee TW, Patrylo P, Zaveri HP. Astrocytes and Glutamine Synthetase in Epileptogenesis. J Neurosci Res. 2018.

144. Boison D, Steinhäuser C. Epilepsy and astrocyte energy metabolism. Glia. 2018;66(6):1235-1243.
145. Binder DK, Steinhäuser C. Functional changes in astroglial cells in epilepsy. Glia. 2006;54(5):358-368.
146. Baker DA, Xi ZX, Shen H, Swanson CJ, Kalivas PW. The origin and neuronal function of in vivo nonsynaptic glutamate. J Neurosci. 2002;22(20):9134-9141.
147. Augustin H, Grosjean Y, Chen K, Sheng Q, Featherstone DE. Nonvesicular release of glutamate by glial xCT transporters suppresses glutamate receptor clustering in vivo. J Neurosci. 2007;27(1):111-123.
148. Kwok CS, Johnson EL, Krauss GL. Comparing Safety and Efficacy of "Third-Generation" Antiepileptic Drugs: Long-Term Extension and Post-marketing Treatment. CNS Drugs. 2017;31(11):959-974.
149. Wyllie E. Wyllie's Treatment of Epilepsy: Principles and Practice. Vol Chapter 43 - Initiation and Discontinuation of Antiseizure Medications. 7th ed: Lippincott Williams & Wilkins; 2020.
150. Noebels JL, Avoli M, Rogawski M, Olsen R, Delgado-Escueta AV. "Jasper's Basic Mechanisms of the Epilepsies" Workshop. Epilepsia. 2010;51 Suppl 5:1-5.
151. Haut SR. Seizure clusters: characteristics and treatment. Curr Opin Neurol. 2015;28(2):143-150.
152. Detyniecki K, O'Bryan J, Choezom T, et al. Prevalence and predictors of seizure clusters: A prospective observational study of adult patients with epilepsy. Epilepsy Behav. 2018;88:349-356.
153. Zheng W, Winter SM, Mayersohn M, Bishop JB, Sipes IG. Toxicokinetics of sulfasalazine (salicylazosulfapyridine) and its metabolites in B6C3F1 mice. Drug Metab Dispos. 1993;21(6):1091-1097.
154. Wahl C, Liptay S, Adler G, Schmid RM. Sulfasalazine: a potent and specific inhibitor of nuclear factor kappa B. J Clin Invest. 1998;101(5):1163-1174.
155. Plosker GL, Croom KF. Sulfasalazine: a review of its use in the management of rheumatoid arthritis. Drugs. 2005;65(13):1825-1849.
156. Sato H, Shiiya A, Kimata M, et al. Redox imbalance in cystine/glutamate transporter-deficient mice. J Biol Chem. 2005;280(45):37423-37429.
157. Buckmaster PS, Haney MM. Factors affecting outcomes of pilocarpine treatment in a mouse model of temporal lobe epilepsy. Epilepsy Res. 2012;102(3):153-159.